SAPIENZA
UNIVERSITÀ DI ROMA

Faculty of civil and industrial engineering

Master of Science in Biomedical Engineering

Design, development and experimental validation of a tactile sensor array integrating FBG transducers for hand biomechanical measurements

Supervisors:

Prof. Paolo Cappa

Dr. Calogero Maria Oddo

Candidate:

Luca Massari

Table of contents

1 Introduction

1.1 Purpose of the Thesis

This thesis addresses the development of a sensorized glove which is part of an entire safety suit, integrated with technology able to sense external forces and body movements and to guarantee comfort. The main application of this device will be in the working environment, for all daily activities where protective garments are needed. These textiles are part of the Personal Protective Equipment (PPE), mandatory for hazardous work tasks especially in factories. Nevertheless they are essential for accidents prevention, more frequent in manufacturing sectors according to the most recent statistics (Eurostat [1], INAIL [2]). These working sectors are characterized by a remarkable occurrence of upper limb musculoskeletal occupational diseases and injuries, and would benefit from the availability of technology able to identify major risk causes and to prevent hazardous behaviors.

The proposed technology will be developed with major attention to its actual deployment in industrial environments and to the regulatory framework. In Italy, the main regulatory source for risks prevention in the workplace is D.Lgs. 81/08 and later integrations [3]. For the analysis of ergonomic risks, the national and international regulatory frameworks mainly refer to two methods: OCRA [4], for the evaluation of repetitive movements, and NIOSH [5] , for the determination of risks for the spinal cord during manual handling of loads.

Although the overall aim of the project is the sensorized safety suit, in this work the main focus is on the development and experimental evaluation of a smart glove, which would be a part of the entire project. [5]

The proposed smart glove, integrated with protective equipment, will have two main functions. The first is the ability to sense external forces (via transducers integrated in the palmar side of the hand) while the second one is the ability to monitor human hand kinematics, posture and gesture (via transducers integrated in the dorsal side of the

hand) for an ergonomic purpose. Hence the glove is intended to improve worker wellbeing by means of interaction and motion monitoring and the subsequent implementation of strategies to limit dangerous repetitive movements.
The smart glove will be equipped with FBG (Fiber Bragg Gratings) transducers [6]. Information from the integrated transducers will in the future be sampled by means of a novel local interrogation unit, featuring miniaturization with respect to properties such as weight, power consumption and physical dimensions, that will transmit acquired data wireless to a remote processing unit.

This technology will also find a field of application in the medical sector, such as in environments for Magnetic Resonance Imaging (MRI). As a matter of fact, in order to monitor patients during MRI, it is necessary that components with metallic parts are not present. Hence fiber optic sensors are an enabling technology because of their compatibility with magnetic fields, which has been already demonstrated in some applications [7]. An interesting point is the fibrous nature of optical fibers that make them perfectly suitable for integration into textiles, [8], that would allow to sensorized wearable technologies such as smart clothes or wearable robots such as exoskeletons [9, 10] and bionic hand or leg prostheses [11].

1.2 Structure of the Thesis

The first chapter introduces the general framework of the thesis and sets the ground for the central part. Starting from the analysis of smart textiles, we introduce the transduction principles of FBG (Fiber Bragg Grating) elements embedded in a fabric.

The second chapter will address the state of the art of smart textiles. This part discusses a selection of pertinent papers, which report about the evolution of the wearable technologies. The presented papers will show both the integration of FBG and FOS (Fiber Optical Sensors) technologies in the medical field and the application to detect movements and body gesture.

The third chapter introduces the design choices of the project. After a short description of the glove, the proposed techniques and materials are discussed.

The fourth chapter shows the experimental phase, where the results of the laboratory trials are explained. The experimental trials and results are discussed in order to investigate the feasibility of the entire project.

The fifth chapter will conclude the study, with a part dedicated to the future expectations of the project.

2 Analysis of state of the art of wearable sensors for hand biomechanical measurements

2.1 Biomechanics of the hand

The human's hand is a tool that can perform numerous actions. Her essential function is a prehensile function and thanks to its architecture it has countless possibilities of location, movement and action. Humans have the thumb that is opposable to all the other fingers, also in monkey the thumb is opposable but have less movement and function. The hand is not just a simple operative organ but is also an exploratory and receptive organ that can transfer to human the information essential to the knowledge of the surrounding world and to its own operation. Without the hand the vision of the world would be flat while the hand with the communication with the cerebral cortex allows to recognize and object without seeing it and to better understand the space around it. Hand and brain are a functional couple that allows the human to evaluate many things.

The fundamental characteristic of the human hand is her adaptability to the shape of the grasped object, for example on a flat surface, such as a glass, the hand come in contact with part of the palm and phalanges. While if the object is big then the hand get bended, making three arches that follow three particular directions. The reference axis of the hand is conventionally coincident with the axis of the third metacarpal and of the middle finger. When the finger are moved away and the hand get open the middle finger remains in his position, while the other fingers move away and the axis of each finger converge at a point located at the base of the hand.

Bones, muscles, ligaments, tendons, veins, arteries and nerves that allow the hand to make complex movements and guarantee multiple functionality, compose the human hand. It has 27 bones and 19 muscles and thanks to his innervation and receptor is very sensitive. The bones are connected each other thanks to the articulations that allow them to perform flexion, extension, abduction and adduction. The muscles may be grouped in intrinsic muscles that are situated in the hand and extrinsic muscles that are

situated in the forearm and are connected to the fingers by tendons. What makes the hand an intelligent and complex organ is the powerful and accurate musculature, the number of bones and articulations and the extremely sensitive epidermis. Human hand is a fantastic example of a natural biomechanical system that is source of inspiration for future robotics projects. The complete system of the hand can be divided in a series of subgroups, these are 1) Structure of the bones, 2) Articulations, 3) Structure of the muscles and 4) Tendons.

Starting with the structure of the bones, the hand have 27 bones divided in three groups: phalanges (14 bones), metacarpal (5 bones) and carpal (8 bones). Each finger is made of three phalanges but the thumb is an exception because has only two phalanges. The metacarpal link the finger to the carpal that link the hand to the forearm making the wrist. The ensemble of metacarpal and of the phalanges of each finger makes a cinematic chain able to move thanks to the action of the intrinsic and extrinsic muscles. The bone segment are link together thanks to the articulations, these last one make possible the relative movements between the various segment and this is why the hand has extraordinary movement ability. The articulations are composed by their joints surfaces (joint capsule, synovial fluid and cartilage) and by the tendons that hold together the different segment bones.

The articulations are:

- Hand’s interphalangeal articulations
- Metacarpophalangeal joints
- Intercarpal articulations
- Wrist

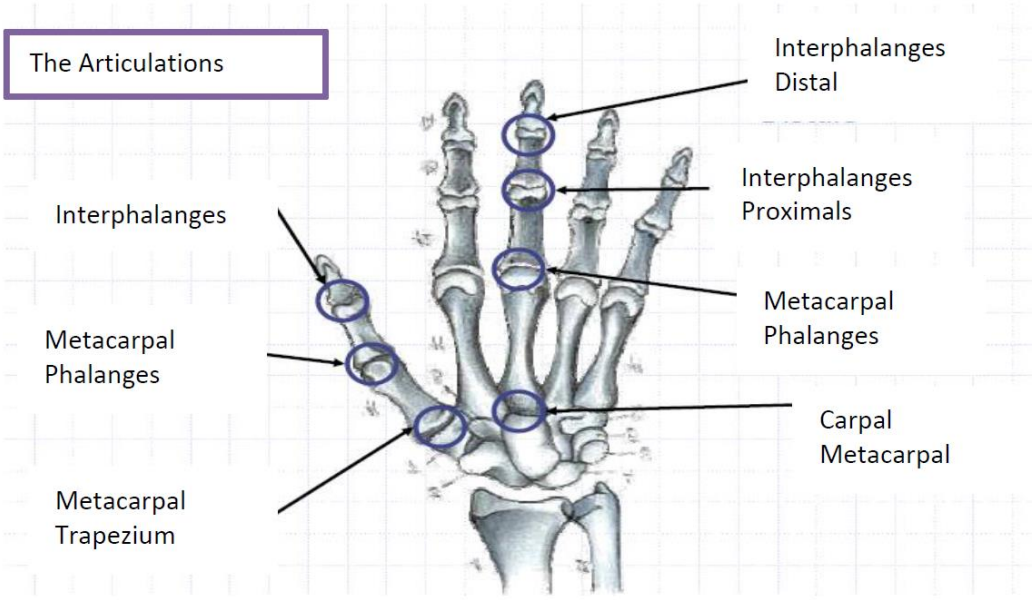

Figure 1 – Bones of the human hand

The human hand has about 40 muscles divided in intrinsic muscles located in the hand and extrinsic muscles located in the forearm. The muscles are composed by fiber able to shortening actively and passively resist to traction bur not able to actively stretch. Thanks to their ability to contract themselves after the command coming from the brain and the spinal cord (CNS - Central Nervous System) they make possible the movements of the hand, by transferring with the tendons the force to the articulations. The fibers of the muscles are linked to the nervous system thanks to the moto neurons; the activation of a moto neuron imply the contraction of a fiber of the muscles. The muscles of the hand are anchored to the articulations with a short tendon located at the proximal extremity and with a long tendon to the distal extremity. The tendons are robust parallel fiber made of collagens that often get through several joints of the hand before going in the bones. Each muscle has his particular and unique function if we consider them isolated from the rest, but when it contracts with the other muscles to realize a specific movement it can be the principal protagonist of that movement ore may try to stop it or may participate in an active way to realize a complex movement. All the muscles of the hand can be considered multi articular because their tendons pass through more than one joint. The actions of extrinsic and intrinsic muscles, always under the control of the brain, allow the grasp and the manipulation of objects. The most fine and accurate

movements of the hand are controlled by the intrinsic muscles, with the collaboration of the most powerful extrinsic muscles of the forearm.

Considering the definition of Degree of Freedom (D.o.F.) and translating it in possibility of movement, the hand has 23 D.o.F allocated among the different joints

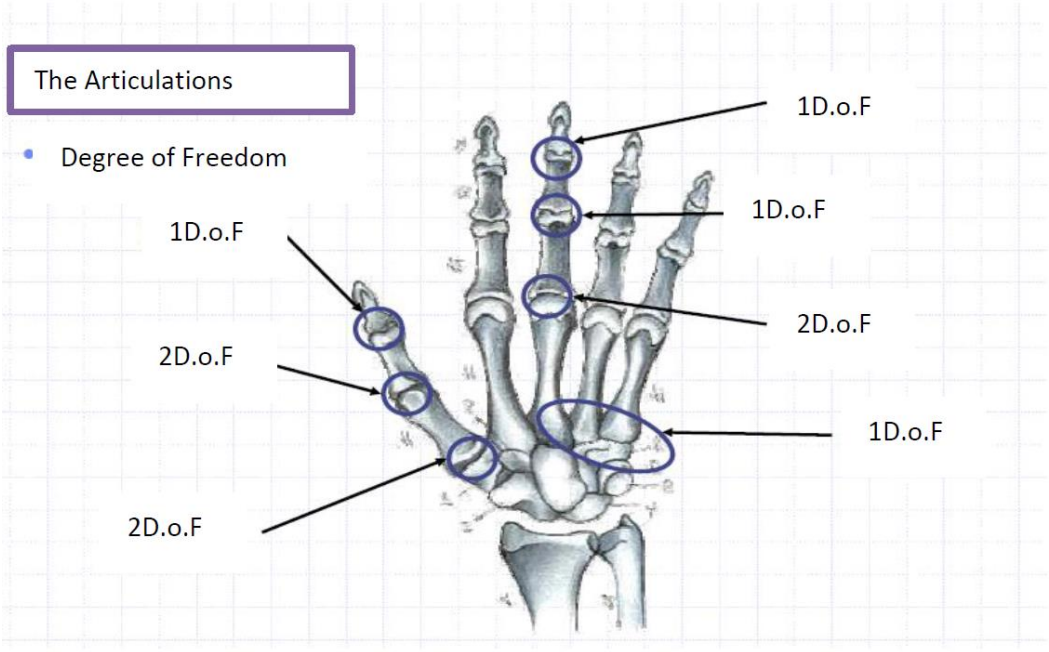

Figure 2 – Degree of Freedom

The flexor muscles reside on the ventral side of the forearm and are arranged on several layers. Among the most important muscles, responsible of the flexion of the fingers, we have the Digitorum Flexor Superficialis (FDS) and Flexor Digitorum Profundus (FDP). The extensor muscles reside on the dorsal side of the forearm. Among the most important muscles, responsible for the extension of the fingers, we have the Extensor Digitorum Communis (EDC).

The intrinsic muscles are divide in interosseous and lumbrical; these muscles ensure, together with the extrinsic muscles, the movement of flexion and extension of the fingers, they are also responsible for the adductions and abductions movements of the fingers.

2.2 Smart textiles

The field of smart textiles has a new growing market that is still in its development phase, thanks to introduction of portable devices and soft computing. These wearable technologies are often used in different fields, starting with the medical and including military, aerospace and commercial applications. This fast evolution of the smart textile is due to the great possibilities which are provided by this technology and of course thanks to the nature of fabrics that makes them perfect for the measurements in direct contact with human body.

Smart textiles are based on fabrics with sensing properties, these are called SFT (smart fabric transducers). The fabrics are sensitive to different stimuli which can be chemical or physical, as example can detect changes in pressure, electrical current, temperature or force. Incorporation of the sensing elements into fabrics generally may be done at different level of integration [12].

As stated before for the realization of smart textiles we begin from the fabrics, which are hierarchically fibrous materials. At the first level of integration there are the fibers, which are the smaller units; these units form the threads which form the yarns, considered as the second level of integration. At the third level of integration we have the fabrics, made from the yarns using different skill such as knitting and weaving. Figure 3 shows the progress of fabric structures from fiber to cloth.

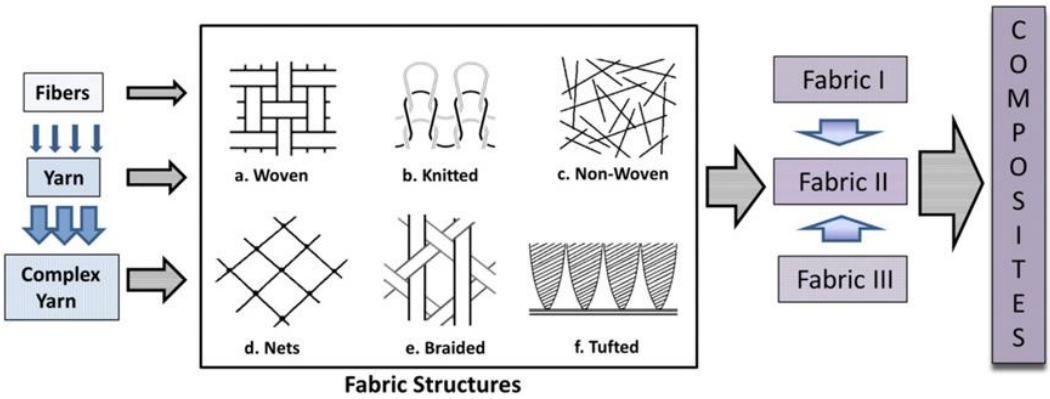

Figure 3 – Fabric construction platform and hierarchy [12]

Every fabric has its own construction, for example knits are more deformable than woven which are generally more hard to deform. In this way it is necessary to pay attention to

the nature of the fabrics because it will determine the type of constituent for an intrinsic integration and the type of bond for an extrinsic integration.

Another interesting factor which has to be taken into account in the construction of the smart textiles is the origin of the fiber units. It is possible to find natural or synthetic fibers, the first one have usually less mechanical compliance and more water absorption (hydrophilic) than synthetic one, which tend to not absorb water (hydrophobic).

This is just an example of the differences between the fibers, but there are a lot more: like susceptibility to chemical reactions, compatibility with coatings, fabrics lifetime and adhesion. It appears evident that the nature of the fabrics is an important design consideration in the construction of SFTs.

Analyzing the substrates of fabrics it results that they can be modified at all levels of the structure hierarchy in order to build an SFTs. At level one, the modification refers to the constitution of fibers; then at level two there is the substitution of the yarns with the sensitized one, an example of this modification are the e-textiles. Eventually there are level three and four: in the former level the modifications request the alteration of the surface of the fabric to give them a sensing ability, whereas in the latter level the modifications imply the use of multiple sensing fabrics in order to form a sensing composite.

2.2.1 Extrinsic modification of fabrics to achieve smart textiles

One of the possible ways to modify the fabrics is to make extrinsic modifications, with the word extrinsic we generally refer to electronic textiles (e-textiles). There are basically two type of external modification, the first involve the attachment on the surface of the fabrics of electronic elements like integrated circuit chips or resistors or self contained sensing elements. The second is the operation of coating, this process imply a plenty of techniques that include screen printing, electrodeposition, sputtering of thin films, vapor deposition and thermoset coatings. As a result of this coating process the fabrics are altered and there is a change in their properties (tensile, bending and shear properties).

2.2.2 Intrinsic modifications of fibers and yarns to achieve smart textiles

Intrinsic modification are different from extrinsic modifications, in this case the fibers themselves are sensitive to some stimuli (chemical or mechanical). Integration became more deeper because the fibers get replaced by sensorized yarns in order to create sensing element from the fabric materials. To list some of the most common techniques of intrinsic modification we can cite electrospinning, self-assembly, wetspinning and die extrusion. However, depending on the purpose of the smart textiles, these intrinsic modifications need to take in account also other parameters such as degree of fabric, density, flexural rigidity and thickness. Smart textiles may be used in some specific application so the characteristics have to be customizable in order to be suitable with the projects.

2.2.3 Pressure and force sensors

One kind of sensors that are more interesting for this project, are the pressure and force sensors, in this chapter there will be a short explanation of those sensors.

To sense pressure and force the ideal vehicle is a capacitive fabric sensor, these sensors are able to detect pressure and are used usually founded in tactile applications. In this scenario is possible to have different materials and designs, they range from intrinsically modified materials to adapted electronics, yet what they have in common is that there is a dielectric element that separates two electrodes. To give some examples, it can be seen that in e-textile are used capacitors that are attached to the fabrics with some method, the most common method to attach the sensors to the substrate is to sew, snap, or glue and then to solder them to the other electronic part or wires. There is also another way to create fabric capacitors and it is from conductive materials that can act as electrode plates and that are separated by different spacers. In case of conductive inks, paints or polymers the plates have to be printed, painted and sputtered, while in case of conductive thread they have to be sewn, woven and embroidered. Soft polymers and fabric spacers may be used to form the dielectrics. Moreover it is possible to create capacitive fibers using techniques like silicon fiber sputtered with metals that can be found in flexible electronics. When fabric sensor capacitors are used in arrays (they can also be used as single elements) they are able to obtain distributed measurements [13].

In this case, the relative capacitance is taken at the intersection of the rows and the columns of the electrodes, which are connected to multiplexer and microcontrollers to DAQ systems.

Furthermore, a mention in this review have to be done for compressible foams, fabrics and polymers. These materials have different advantages, but also some concerns like poor resilience, hysteresis and signal drift. These issues can be negligible in some particular condition like small usage and small operating range. The outputs of capacitive fabrics are generally nonlinear, with some exception where it is possible to find regions of linearity. Parameters such as temperature and humidity have some effects that are not well addressed and have to be studied. The possibilities to build fabric pressure sensor are several, one of them is to find a correlation between electrical resistance and pressure. When a pressure is applied in a specific point there is a change in the contact resistance of the intersecting yarn, this location can be defined by detecting the position where the change of the resistance occurs. One of the advantage of these sensors is that can be create at all the structure level, that means fiber, yarn, thread and fabrics [14]. Analogous sensing principle can be found when the resistance between conductive elastic yarns increases due to an applied pressure, this happen when the yarns are woven [15].

Cu-Ni electroplated polyester conductive fabric is also another type of pressure sensor which is made from a combination of sheets of conductive textiles and conductive yarns. In this example the layers are divided by a grid of sensing elements which operate as discrete electrical switches [16]. The plates on the opposite sides of the net (which form the grid) come in contact when there is a pressure that is enough to generate a contact event. To have a measurement of the pressure that is applied is necessary to count the number of regions that are activated. Relevant is the way of creating pressure sensitive fabrics by coating them with pressure polymers, an example are the small pieces of piezoelectric material embedded in conductive silicon.

Lastly, it is significant to notice that most of the commercial capacitive devices found their application in the medical field.

2.2.4 Discussion of smart textiles

This part has provided a review of SFT technologies. It has been discussed the difference between intrinsic and extrinsic modifications, while the first deal with sensing fibers the second deal with electronics components sewn to the fabrics. While intrinsic elements come from doped or conductive polymers, extrinsic elements are coatings or discrete units. Both the modification have the objective to give sensing properties to the textiles such as resistive, capacitive or optical characteristics. It has also been explained the use of the fabric pressure sensing capacitors, these sensors have generally a capacitance in the order of picofarad, depending on the application there are several different geometries and usually the plate layers have a thickness that goes from microns to millimeters.

There are many factors that have to take in account when designing and developing a smart textile transducer, in Figure 4 there is explained the different key areas that have to be considered. All the different options have to meet the requirements of the application, in order to create a unique solution for the purposed objective.

In the future smart textiles will have more importance thanks to their outstanding potential, but for now there are still some drawbacks that have to be considered, in fact the main concerns for an expansion of the smart textiles are:

1- Lack of standards
2- Lack of reliability
3- Expensive cost
4- Lack of mass availability of components

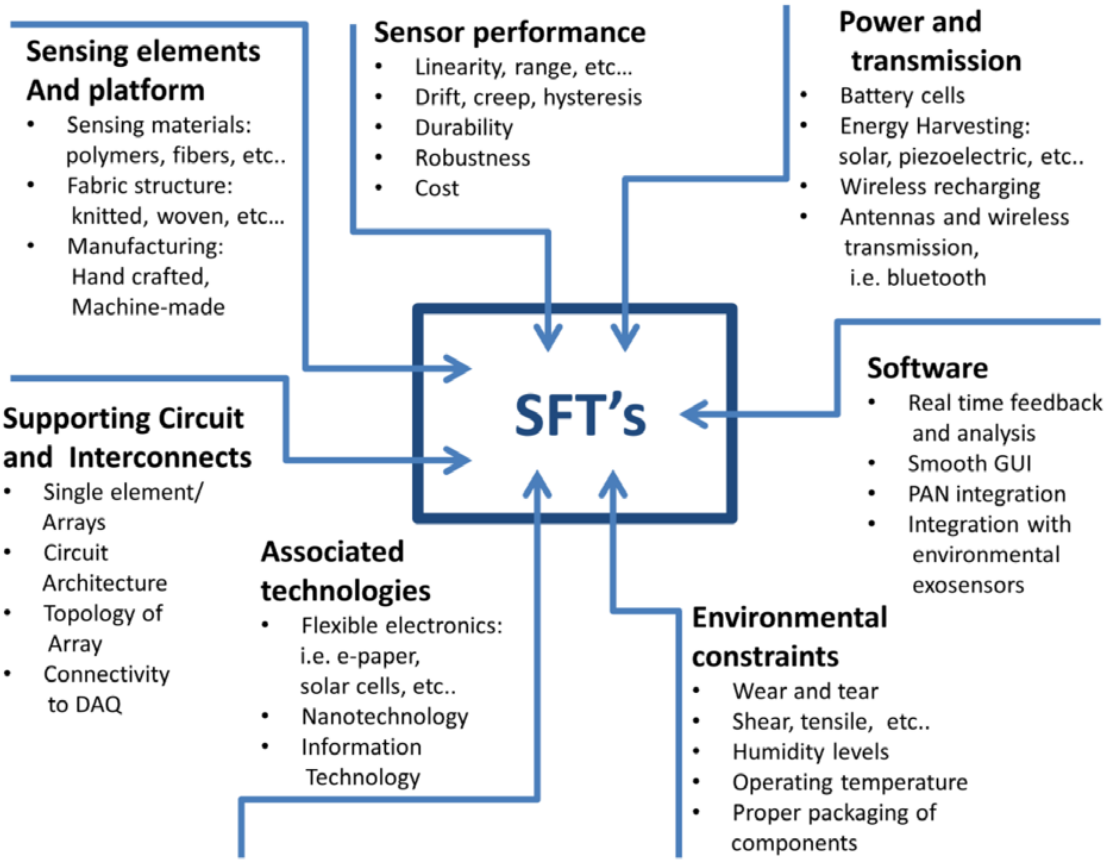

Figure 4 – Key areas of development of SFTs [12]

2.3 Optical fibers

Smart textiles are used in a wide range of applications (civil engineering, transport), but also in the field of medicine, in particular it is of great importance the monitoring of physiological parameters like heartbeat and respiratory activity. In healthcare applications appear very relevant and important the continuous monitoring of the patient. Of course, there are several approaches and different possible devices available, but using optical fiber integrated in smart textile offer many advantages.

One of the biggest advantage is the possibility to create MR-compatible systems. Considering different medical branches (surgery, orthopedics, neurology and cardiology) there is an increasing request for MR procedures, so as effect there is also a necessity of systems that can be used in a MR environment, systems able to monitor the patient physical parameters in order to provide real time feedback about the status of the

patient. Smart textiles that use optical fibers can be used with excellent results in the healthcare monitoring.

It might be very useful to have a lightweight and small size system, that could allow a normal range of motion of the patient and preserve his comfort. In homecare applications, one of the most important feature is the privacy of the patient, for this reason is generally recommended to use enclosed rooms and to transmit the data over secure lines.

Conventional sensors have many electrical connections that may be dangerous for the patient, while optical fibers are safer and may be used to monitor different physiological parameter in MR-procedures. Also in the case of using optical fibers is important to find a solution for the connection of the fibers, several solutions are available since it is very significant that the connectors are properly designed for MR-procedures. Furthermore, smart textiles integrating optical fibers are comfortable and easy to wear for the patient, this achievement seems relevant to improve the quality of life for the patient. In this way it looks quite easy to have a system, which is not either dangerous or uncomfortable, able to continuous monitoring the physiological parameters.

Among all these advantages there are also some drawback. As stated before one of the main concern is the problem related with the connections of the fiber during a MR-procedure, but there are also some problem due to light coupling, especially when considering long-term applications at home, in fact the stability has to improve in order to fix this issue. Another minor problem is related to the washability (and sterilizability) of the smart textiles integrating optical fibers. Due to the expensive cost of these devices is not possible to use them for one patient, therefore this problem have to be face and future studies should resolve this issue and increase the durability and the robustness of these smart textiles against water and soap.

Thanks to the good results obtained by these optical fibers, further studies are motivate to find solution for the improvement of the quality of the component and the reduction of their cost. The goal is to achieve a massive use of these smart textiles and a more availability in commerce [17].

2.3.1 FBG (Fiber Bragg Gratings) Principles

The use of optical fiber as sensing elements is a new and evolving field that give great potential in order to find solutions for monitoring and measuring, in an accurately way, strain, shear and contact skin pressure. There are many advantages by using light for sensing measurements since light propagation is very sensitive to external forces. Other interesting advantages offered, are the possibility to have real-time measurements with almost negligible hysteresis, to have immunity against electromagnetic interference, to have a small size and low weight system, to have the possibility to parallelize the readout, to have passiveness and last but not least to have resistance to harsh environment.

There is a wide range of different optical fiber sensors, in fact it is possible to use light for measurements in many different ways starting from scattering sensor to interferometers. Among this variety of sensor, there is one that has particular influence and has been object of paper and review in the last years, the FBG sensor (Fiber Bragg Gratings).

FBGs are optical fiber-based sensors, which present all the advantages related to optical fiber sensors. The main feature is that the FBGs are sensitive intrinsically to strain and temperature. These sensors are very useful in wide range of applications, in particular they can be used in an optimal way in the field of smart textiles since their fibrous nature. It seems evident that FBGs are the right choice for the sensing glove.

To explain the working principle of a FBG sensor it is useful to introduce the Bragg signal, when the light pass through the grating, part of the signal is reflected; this part is function of the strain and the temperature suffered by the sensor, so its spectral component change with different conditions. Each FBG occupies a small bandwidth, this is important when the number of sensors on the same fiber increase because as effect the spectral range available decrease. An interesting point is that FBGs can be easily multiplexed in a serial distribution along a single fiber, of course there is a limit of the numbers of gratings that can be putted on the same fibers and it depends on the dynamic range.

The Bragg wavelength condition is given by the expression:

$$\lambda_B = 2 \cdot n_{eff} \cdot \Lambda_B \quad (1)$$

where Λ_B the grating pitch and n_{eff} the effective refraction index of the fiber core. To analyze the Fiber Bragg Gratings properties it is necessary to inject light from a spectrally broadband source into the fiber, what happens is that a narrow part of the light is reflected back and another part is transmitted; these effects occur when the light reaches the gratings (Figure 5). As stated before FBGs are sensitive to strain and temperature and these two parameters influence the spectral reflection which can be measured with an interrogation unit. The response is both defined from the physical elongation of the sensor (and the corresponding change in the pitch) and the change in fiber index due to photoelastic effects, this last effect arise from the thermal expansion of the fiber material.

Thanks to the equation (1) appear evident that the wavelength component of the reflected signal λ_B change according to any variation of the mechanical or physical properties of the grating region. When strain is applied, there is a change of Λ_B and n_{eff}, in the same way when temperature changes it bring to a variation in n_{eff} due to the thermal effect.

In an unconstrained fiber, Λ_B is influenced by thermal expansion or contraction. Equation (2) correlates this FBG behavior. The first equation term provides the strain effect on λ_B while the second describes the temperature effect.

$$\Delta\lambda_B = \lambda(1 - \rho_a)\,\Delta\varepsilon + \lambda_B\,(\alpha+\varepsilon) \quad (2)$$

where $\Delta\lambda_B$ is the change in Bragg wavelength, ρ_a, α and ε are, respectively, the photoelastic, thermal expansion, and thermooptic coefficients of the fiber, ΔT is the temperature change and Δε is the change of strain. To give an example of typical values for an FBG written in a silica fiber in a polymeric foil and with λ_B=1550 nm, the sensitivity to strain and temperature is approximately 8 nm per 1% of elongation and 0.1 nm/°C, respectively [18].

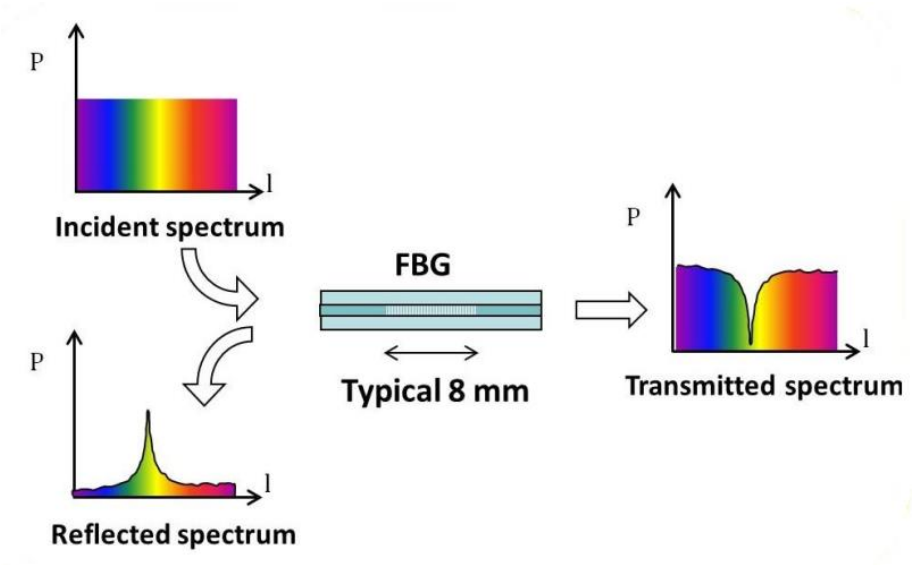

Figure 5 – FBG measurement architecture [50]

2.4 Smart textiles based on Optical Sensors

Research on smart textiles integrating optical fiber is an active field of study for different groups around Europe, but the most relevant paper were written by the people involved in the European project called OFSETH (optical fiber sensor embedded into technical textile for healthcare). The main objective of this project was to create smart textiles embedded with optical fibers in order to monitor different physiological parameters. In this work are presented the applications of smart textiles based on FBG sensor and smart textiles based on intensity modulated FOSs (Fiber Optical Sensors)

2.4.1 Smart Textiles based on FBG Sensors: Medical Applications

Due to his properties FBGs are generally used for technologies based on the measurement of the strain sensed by the gratings. Designing a smart textile integrating FBGs allows the monitoring of several parameter of physiological interest, an example is the monitor of the respiratory movements. In the past some research demonstrated the usability of FBG sensors in order to detect respiratory movements and the breathing rate [19, 20], but only in the last year they have been embedded in smart textiles.

Thoracic movements are smaller than abdominal ones therefore it is a necessity to have a system able to discriminate small strain, the sensitivity of a FBG (≈1.2 pm·$\mu\varepsilon^{-1}$) is enough to sense them [21].

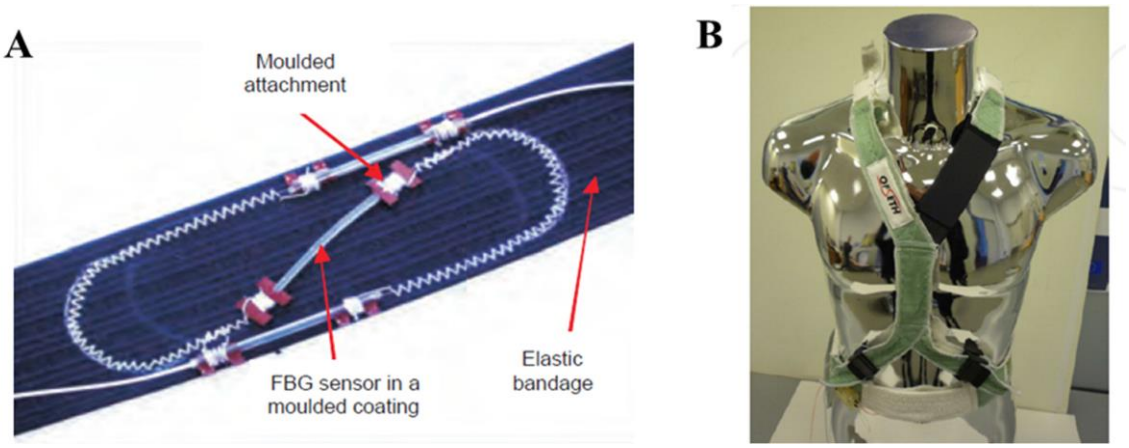

Figure 6 – (A) Design of the FBG sensor developed in OFSETH project; (B) MRI-compatible sensing harness which embeds the fiber optic sensors for the respiratory monitoring [21]

In the experiment showed in Figure 6A there is one FBG embedded by stitching to the textile, in order to do the calibration of the system the textile has been stretched in step of 0,4% up to 40%. 0,8% was the value of strain experienced by the FBG, of particular interest is that the system performed good linearity from 8,5% to 35%-40% of textile stretching, with a sensitivity of 0.35nm/% and an accuracy better than 0,1% of elongation. Long term properties may also have an important value in order to analyze the stability and have been carry out some trials to evaluate this characteristic in [22]. The sensor has performed 90,000 cycles in 129 hours in order to test the mechanical robustness of the sensor, these trials were taken with a simulated breathing rate ranging from ten breaths per minute to twelve breaths per minute. In (Figure 6B) is showed a particular belt that provide access to all vital organs of the patient while providing the continuous measurement of the respiratory movements.

FBG sensors can also successfully be employed to detect both the heart rate and the respiratory cycles, this experiment has been perform in a recent paper [23]. This article showed some interesting innovation referred to the structure, in particular in this work the FBG sensor was embedded in a PVC laminate. The process was handle by an spread-coating process that create this strain-sensitive foil, which performed at the end of the process a sensitivity of 0.8 pm·$\mu\varepsilon^{-1}$. To test the new sensor some trials were performed on healthy volunteers, in the trials have been used two different filters, one for cardiac frequency monitoring and one for breathing rate monitoring. The first filter was a band pass filter in the range of 0.5-1.3 Hz, while the second was a band pass filter in the range of 0.1-0.4 Hz.

One of the main drawbacks of the FBG is the simultaneous measurements of temperature and strain, nevertheless various devices able to detect decouple the two quantities were shown, such as a system for measuring cardiac frequency and breathing rate over a wide range of temperatures [24]. Polychloroethanediyl was chosen as material in which the FBG was embedded, this polymer was chosen thanks to its good sensitivity to strain and his good performance/cost. In addition, this system (for elongations in the 0.6% to 1.6% range) showed a linear response. Analyzing this range the FBG sensitivity was about 8 nm/% because the FBG showed an increase of about 8

nm. The cross sensitivity (temperature – strain) was fully evaluated within this study and it was found an increase in the wavelength of Bragg of about 10.7×10^{-3} nm/°C, that mean that there was a change of 1,5 nm for a temperature increase of 140 °C.

The group of Dziuda has also proposed a solution to monitor respiratory movements and heart activity, their system consisted in a Polymethyl methacrylate (PMMA) board. The size of the board was 220 x 95 mm^2 and its thickness was of 1.5 mm, with the help of epoxy adhesive an FBG sensor was attached to this board [25]. What they have experimentally evaluated is the error of the system in the measurements of heartbeats per minute and breaths per minute when MRI (Magnetic Resonance Imaging) examinations are performed. The results were very good and showed about three heartbeats per minute and one breath per minute. The development of two FBG sensors positioned perpendicular to each other was also evaluated from the same research group [26]. In order to validate their systems under MRI procedure it was necessary to compare the results of their sensors with the results of an MRI compatible portable module, the research group made the trials on three patient [27]. Also in this case the results were good showing a low relative error (about 8%) that can be considered small because this system is specific for monitoring and not for diagnosis. Lastly, always considering the same research group they have studied a new system for the monitor of heart rate which is MR compatible and has already been tested. The trials were taken on seven healthy volunteers and the results showed a root mean square error of less than six beats per minute [28].

In the field of monitoring of the respiratory movements is interesting the work of Allsop and coauthors, they developed a wearable system [29] made of an array of 40 FBG sensors. These sensor were in a line an each sensor consisted in two FBGs in order to produce 20 curvature sensors in several different locations. What was evaluated from the experiments was the ability to measure the absolute volumetric changes of the human torso (the estimated error was about 6% on the average volume).

Moreover, is important to cite the work of Li and coauthors, which developed an intelligent wearable system based on FBG for the monitoring of human temperature [30]. Their systems start from partly embedding an FBG in a polymer filled strip in order

to improve the sensitivity, the final work showed a big improvement in temperature sensitivity (150 pm·°C^{-1}), in fact it was almost 15 times higher than that of a bare FBG. Their systems consisted in five distributed FBGs placed in five different positions in order to measure the human body temperature, an example of the locations of the FBGs is chest, right and left, armpit right and left and center of the upper back. From the data collected by this five FBG they developed a model to calculate the human body temperature with an accuracy of ±0.1 °C.

To capture hand gestures and posture the group of Silva and colleagues developed a wearable sensing glove (Figure 7) [18]. This glove is also based on the use of FBG sensors, thanks to their multiplexing and self-referencing capability that makes fiber Bragg grating suitable for this application. The glove will have just one optical fiber that have to cross all the hand, but of course there will be more than one grating. The FBGs will be putted in specific places, like the finger joints. The main advantages of this system is the simplicity that makes it suitable for therapy applications. Other fields of application for this glove may be in the virtual reality, the remote control application, or even the study of the human kinematics during sport.

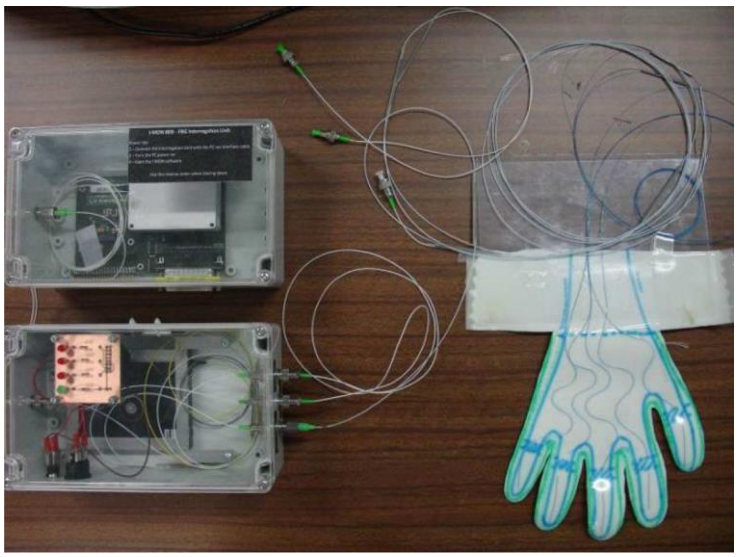

Figure 7 – Glove's optical setup [18]

Within this study the performance and the functionality of the glove was evaluated. The results showed linear response for the movement of closing and opening the hand.

Thanks to the sensor response it was possible to get many information, starting from the joint angles it was also possible to estimate the finger force but also to provide numerical data about the angles of the hand posture in real time. A crucial step is the process of embedding the optical fiber sensors with the FBGs in a flexible polymeric foil (this process has been previously studied by the same group [31, 32]). The so obtained polymeric foil have characteristic of stretchability, flexibility and the capability to maintain a good bonding among the optical fiber and the substrate. Three layers composed the final structure of the polymeric sheet plus the optical fiber with a final thickness of 900 μm. The fiber with a 250 μm diameter was embedded in the middle layer and then were added the superior and the inferior substrates. It was important to assure the bonding and the stimulus transfer, so it was necessary to use a material able to ensure such properties, PVC with a specific formulation was the final choice. One of the advantages of this structure is the possibility to fully customizable the prototype, so it was created a special configuration with the shape of a hand, which was made from a standard textile glove.

The base foil shape was a letter sized foil in which a hand shape was drawn and the fibers were positioned. The successive step was to cut the foil maintaining the shape of the glove and then to sew it to the top face of a standard fabric glove. The final product was made trying to respect the finger movements, from which there were obtained the linear results while performing the opening and the closing of the hand. Thanks to the linearity of the system it was easy to get useful information about the hand posture and the range movement. Silva et al developed also a program that run in LabVIEW to monitor the hand in real time. This program could provide a virtual hand model for 3D visualization, but also provided information about the angle of the joints where the sensor were placed. The possible applications for this glove are in the physical therapy but non only, another interesting thing offered by this system is the valuable output not only for the therapist but also for the patient, who is motivated with interesting exercises and can see his progress on the monitor.

Kanellos et al [33] report on the development of a flexible 2D optical fiber based pressure sensing surface suitable for biomedical applications. This pressure sensor is based on FBG technologies, in fact in the sensor there are several high sensitivity Fiber Bragg Gratings

elements that are embedded in a thin polymer sheet in order to form a 2x2 cm^2 sensing pad with a minimal thickness of 2.5mm (Figure 8). One of the characteristics of this system is the portability, this issue was take in account by associating to this sensor a low physical dimension interrogation unit. The sensor performed a pressure sensitivity of 12 Mpa^{-1} with a spatial resolution of 1x1cm^2 while demonstrating no hysteresis and real time operation. This system showed some very attractive properties that may be useful in several biomedical applications in which is important to measure the pressure, an example could be amputee sockets, wearable sensors, wheelchair seating-systems, hospital-bed and shoe sensors.

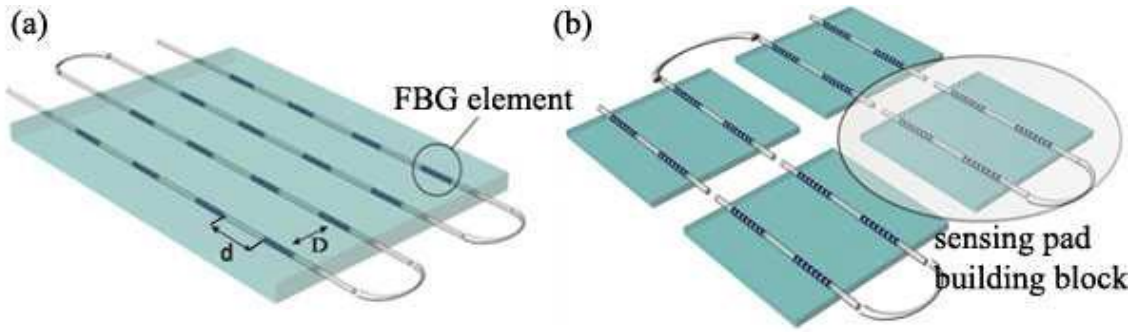

Figure 8 – (A) PDMS 2D sensing surface with FBG-array optical sensing elements; (B) elementary 2D sensors used as building blocks for large scale surface sensors [33]

The creation of this 2D pressure sensor followed a specific procedure, the foiled optical fiber sensor elements are embedded in thin silicon polymer (silicon-polymer Polydimethylsiloxane (PDMS)) material to form an elastic sensing sheet. As shown in the above figure the axial spatial resolution is defined by the longitudinal spacing *d* .The final pad has some useful fields of application because it can be wrapped, embedded or attached to many objects in order to measure mechanical variation such as pressure, deformation and strain on the entire surface. To assure these properties the pad where the optical fibers are embedded has to be flexible and stretchable.

2.4.2 Smart Textiles based on intensity modulated FOS sensors: Medical Application

In this section, it is introduce another type of optical fiber, the so called intensity-modulated FOSs. These fibers are able to modulate the light intensity that is measured by other elements for example a photodiode when there is an outside effect. To better understand the principles of that sensor it is helpful the Figure 9A. In the figure are showed two optical fiber at a variable distance (*d*), what happens is that the intensity of light on the second fiber is lower than that on the first fiber, that is because light expands into a cone of light so there is an obvious loss depending on the distance. In this way it is possible to consider the light intensity as an indirect measurement, what is calculated is the distance between the optical fibers, but also all the variables that may influence the distance. Analogous configuration is the one in Figure 9B, where has been used a mirror an just one optical fiber, but the principle of function is the same of the previous experiment and depends on the distance from the mirror.

Furthermore, another interesting configuration is the one that take advantage of the principle that explain what happen when the optical fiber is bent. Bending the optical fiber with a particular radius imply a loss of light that is travelling from the core to the cladding, the result is that there is an interesting intensity modulation of light going through the fiber (Figure 9C). These sensors are called macrobending sensors and are based on hetero-core fibers that have been studied in several research in order to measure different physical properties [34, 35].

In the 1965 Lindstrom and Lekholm developed an intensity modulated FOSs for medical application, their purpose was to create a sensor to monitor intravascular pressure [36]. To monitor the intracranial pressure it was developed a similar sensor (always based on FOSs), this sensor was manufactured by Camino Laboratories Inc. it seems evident that these sensors have found their field of application for the monitor of pressure and temperature [37]. Introducing the medical application of macrobending FOSs, we found that most of them deal with the monitoring of respiratory movements [38]. Of relevant importance is the fact that these sensors are very common in smart textiles, in the next paragraph there will be a review of the medical applications integrating FOSs.

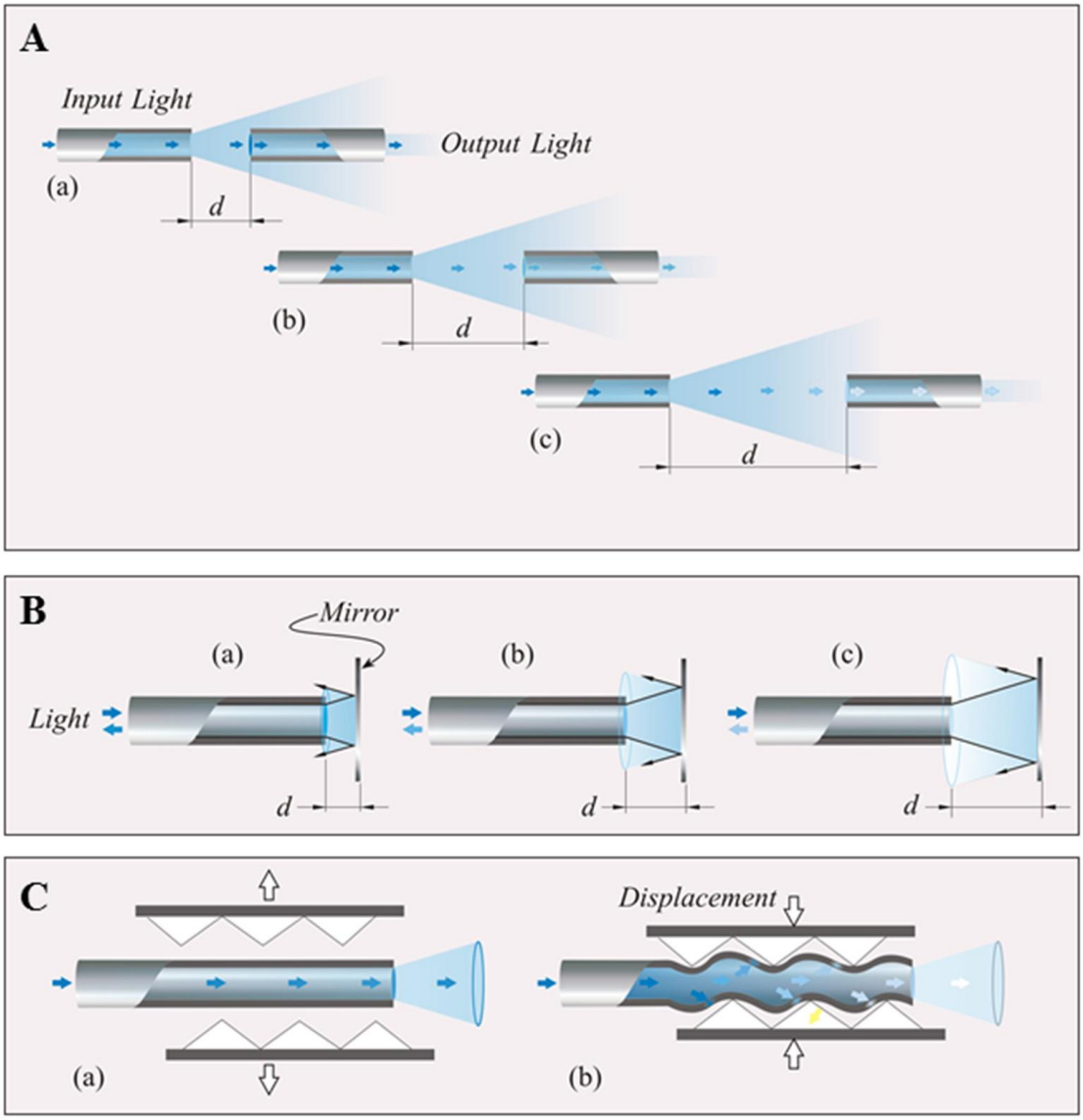

Figure 9 - (A) Schematic of the working principle of an intensity modulated sensor using two fiber optic; (B) schematic of the working principle of an intensity modulated sensor using a fiber optic and mirror; (C) schematic of the light lost from the fiber [17]

In recent year, the number of smart textiles based on intensity modulated FOSs (especially macrobendings) has grown up, these smart textiles were principally used in the monitoring of physiological parameters. Also the researches of the OFSETH group were involved in smart textiles based on FOS, in particular using macrobendings FOS for the measurement of the respiratory rate on the patients that were going under MRI procedures [39]. In order to be compatible with MR, the devices were putted out of the magnetic resonance influence and the sensor itself was suitable to work in this environment. In the figure below is explained and showed a single mode fiber that was embedded in a textile, this macrobending sensor was used to check the movement

abdominal. In this case were not used the FBGs because since the abdominal movements are larger than thoracic one, macrobending FOSs which have lower sensitivity may be employed without using gratings that are even too sensitive for this application (Figure 10). To fix the problem of the large oscillations of the sensor output that were found from the research group during the stretching of the textile, it was decided to developed a sensor with more period of the U-shape, that change could allow the right measurement of the breathing rate. Thanks to this configuration the sensitivity of the sensor increase, to make an example when there was a textile elongation of 38%, the response of the sensor increased from a single-loop design to a 10 loops-design, in number from 3 dB to 28 dB.

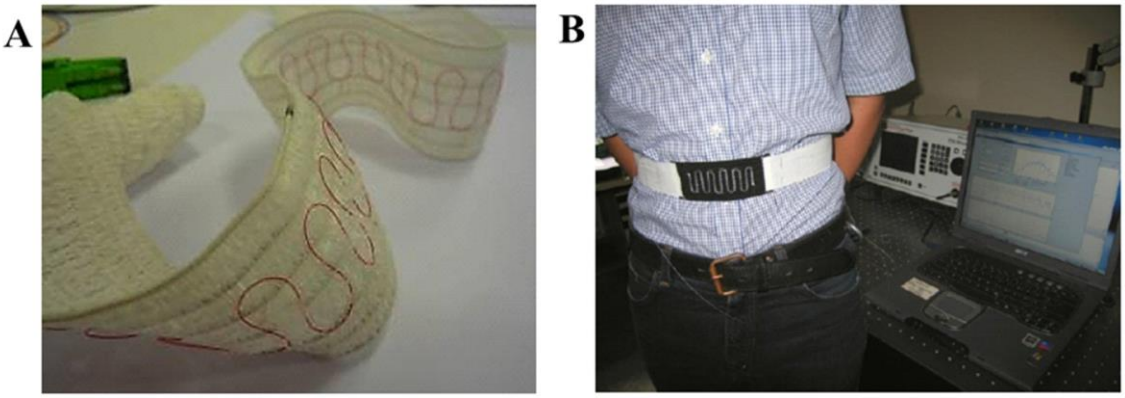

Figure 10 - (A) Textiles based on macrobending FOS embedding a standard single mode fiber; (B) Macrobending sensors for monitoring of abdominal movements [17]

Remarkable is the work of Krehel et al, they designed a smart textile for respiratory monitoring that was based on FOSs. When a pressure (or force) is applied on the fiber what happens is that the geometry of the optical fiber change as it fell the pressure, next there is a light loss in the optical fiber due to the geometry changes that change the wave guiding properties. This type of sensor has been explained in [40], the results showed that the applied force up to 40 N on 3 cm of fiber length was measurable with a threshold of 0,05 N. In order to study the feasibility of the wearable system they decided to make trials at two breathing rates and at different positions of the sensing element on the human body. Using the Bland Altman analysis it was possible to make the comparison

between a normal device and these sensors. The results explained that the several differences among the two type of measurements were concentrated in the range $\pm 3 min^{-1}$, and the limits of agreement were about ±6 min^{-1}.

2.5 E-Textiles

This section will analyze a selection of studies discussing about E-Textiles, their use and their applications.

Tognetti and colleagues [41] studied an innovative category of devices that use conductive fibers meshed with elastic textile fabrics (Figure 11). They have presented in their paper a different type of sensor (strain sensors), these sensors are an optimal compromise among mechanical transduction and integration into textiles. What is presented within this study are the so-called conductive elastomer (CE), this material showed piezoresistive property under pressure or when a deformation is performed. In simple word when an object change his shape, the sensor that is attached on it also change his shape being stretched. When this phenomenon occurs the sensor change his electrical capacity due to this modification and this can be measured in an accurate way. One advantage of the CE (Conductive Elastomer) is that they can be applied on fabrics or to other flexible substrate and can be used as strain sensors. Tognetti decided to realize a smart textile integrating the CE sensors into the fabrics, his idea was to developed a wearable textile able to detect movement and posture. In fact this paper explain the realization of such wearable sensing textiles, the objective was to make an entire set of cloths. In order to give value to the project, the result were compared with the results obtained from a more traditional tracking system. Analyzing the body segment position reconstruction, these smart textiles have displayed very good and encouraging results. Starting from an adhesive mask that had the shape and the dimension of the designed sensor, Tognetti integrated this adhesive on a lycra textile or on cotton and then realized the final sensor by smearing the CE.

What comes out from this research is the possibility for wearable textiles to be used as a valid alternative in some rehabilitation application or sport. This achievement was possible thanks to the fulfilment of the comfort and the wearability, in particular the use

of garments without obtrusive metallic wires is a crucial solution for a long-term use and as consequence a continuous monitoring.

Figure 11 – Particulars of the sensorized glove. Sensors and connections to the electronic acquisition unit are made by using CE. Metallic wires are needed only in the periphery of the glove. In this way, movements of the hand are unbounded [41]

Another interesting work is the one of Lee et al [42], this team has recently (Feb 2015) demonstrated an efficient textile based pressure sensor with remarkable and very good properties such as high sensitivity and excellent durability, moreover the sensor performed a very fast response and a relaxation time based on the conductive fibers coated with dielectric rubber materials.

The advantages of a capacitive pressure sensor are that they have a simple design, high sensitivity, stability and low power consumption [43]. In general, to realize a textile based capacitive pressure sensor, two conductive fabrics are used as electrode plates and are used soft polymers or foams as dielectric spacers due to their flexibility properties. Of course there are also different drawbacks in the use of capacitive pressure sensor, to make an example these sensors have poor resilience and sensitivity. These concerns are mainly caused by the low electrical conductivity of the fibers and also from the bad mechanical properties of the dielectric polymer layer. The objective of Lee was to realize a high performance pressure sensor embedded in textiles, high performance mean excellent electrical conductivity and excellent stability against outside phenomenon like

external deformation. To make this possible several methods have been studied, starting from dip-coating process of carbon based material to electro plating process. However the above mentioned methods are limited and cannot reach the required electrical and stability standard at the same time. While carbon based conductive fibers realized from the dip-coating process have excellent stability but poor electrical properties, the metal based conductive fibers realized from the electro plating process are the opposite (low stability but high electrical properties). In their paper Lee and coauthors decided to use an innovative chemical process, in this way the fiber were coated by applying a specific polymer on the surface of the Kevlar fiber, the polymer in question is poly(styrene-block-butandien-styrene) (SBS). After the coverage there was a conversion of a huge amount of silver (Ag) ions into Ag nanoparticles directly in the SBS polymer (Figure 12).

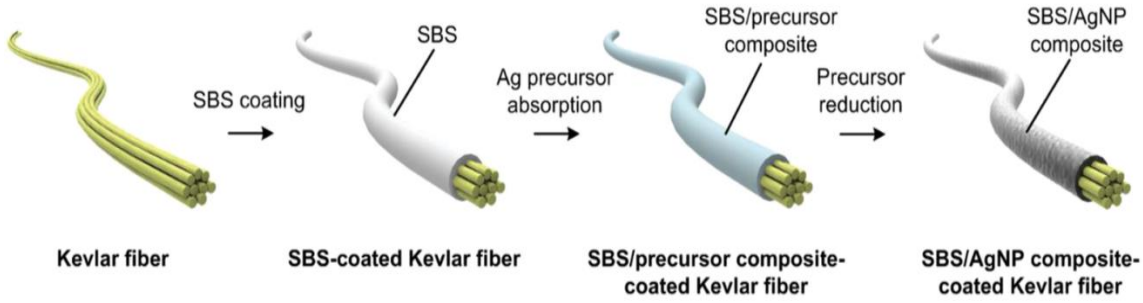

Figure 12 – Schematic illustration of the fabrication of a conductive fiber [42]

The procedure involved three principal actions: 1) coating of SBS on the surface of Kevlar fiber, 2) absorption of Ag precursors into the SBS layer, and 3) reduction of the Ag precursors to form Ag nanoparticles in the SBS layers. To obtain a uniform coating on the surface of the Kevlar fiber of the SBS polymer the flow was perpendicular to the ground [44]. Another crucial step is the absorption of the Ag precursor into SBS layer, to realize this the coated fiber was putted in a 15 wt% $AgCF_3COO$ solution in ethanol for 30 minutes. Thanks to this it was possible to have a rapid and effective absorption of the Ag precursor but also the absorption of the alcoholic solvents into the layer of SBS due to the interaction among the CF_3COO^- (trifluoroacetate anions) and –OH of the solvent alcoholic (hydroxyl groups) [45]. The Fourier-transform infrared spectroscopy (FTIR) was used to identify the amount of absorption of precursors in the SBS layers, in order to measure this increment it was necessary to analyze the fiber before and after the

absorption of the Ag precursors. The results showed two peaks in the FTIR graph, the first at 1130 and the second at 1184 cm^{-1}, these peaks indicated the presence of the C-F stretching. That is enough to reveals the big absorption of the AG precursors inside the layer of SBS polymer [46]. The absorbed Ag precursors were reduced using a solution of hydrazine hydrate ($N_2H_4 \cdot 4H_2O$), to generate Ag nanoparticles inside the SBS layer. The Ag nanoparticles demonstated an excellent connection among each other,, this mean that these particles were coated in a densely way on the SBS layer having 70-90 nm diameters and having a perfect connection between each other. Nearly all of the Ag precursors absorbed in the SBS layer polymer were effectively converted to Ag nanoparticles also in the layer.

The so realized conductive fiber had amazing properties such as good electrical property (0.15 Ω cm^{-1}) but also good stability against external deformation. The excellent electrical properties are due to the dense electrical connection of the Ag nanoparticles and the stability have been evaluated in a 3000 bending test. The last step was the coverage of the obtained fiber with dimethylsiloxane (PDMS), this polymer was used as dielectric layer and to stack the two PDMS-coated fibers perpendicular to each other. Eventually a capacitive pressure sensor integrated in textile was successfully realized (Figure 13). The obtained pressure sensor exhibited high sensitivity (0.21 Kpa^{-1}), high stability over more than 10000 cycles and very fast response times in the millisecond range. One of the applications of this sensor is the possibility to be embedded it into gloves and clothes to control machines via wireless.

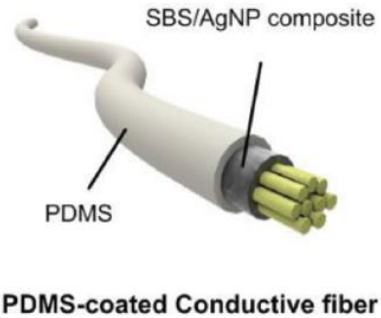

Figure 13 – Schematic illustration of the fabrication of the pressure sensor [42]

The last paper presented about E-Textile is the work of Carbonaro et al [47], in this article is presented an original wearable glove realized with knitted piezoresistive fabric (KPF) sensor technology. The aim of this glove is the capture of hand movements and gesture and this is realized by using KPF in a double layer configuration in order to let it work as angular sensor (electrogoniometers).

To track flexion and extension movements, in particular the one of metacarpophalangeal joint of thumb, index and middle finger this glove has been provided with three KPF goniometers. People that survive to stroke need a period of rehabilitation and during this period is important to monitor the patient in their daily-life activity. To test the feasibility and the results of the project, the glove has been studied in comparison with another tracking system (in this case an optical system). The optical system was considered to be the gold standard both for dynamic and static measurements of the gesture of the hand. The results were promising and interesting, in fact the angular error, made with the Bland Altman analysis [48], has been estimated ± 3° which is slightly less accurate than commercial electrogoniometers. Another interesting advantage is that the output of the KPF goniometers is independent from the bending profile and this make possible to not take in account difficult calibration procedures. All these properties and characteristics make this device suitable for the detection of human movement. The project presented many drawbacks that have been evaluated in this study, for example there is the problem of the limitation in terms of type and number of sensor connections that could avoid the mechanical constrain given by the metallic wires and thus improving comfort.

Future works will be aimed at further assessing the sensing glove capabilities in terms of tracking patient hand function in daily-life conditions, with special focus on stroke patients. In addition, the technology which consented the development of both sensors and connecting wires using KPF materials will be improved to optimize the sensor spatial resolution and enable the possibility of using goniometer networks for monitoring the complete set of the hand joints.

3 Design and development of a sensorized glove integrating FBG transducers

3.1 Glove layout

The aim of this project is to achieve a sensing glove simpler and more easy to use in comparison with the competitors. This goal is take in account by realizing a wearable textile that can ensure minimum issues when worn continuously. The system has to work via optical fiber and have to be very simple.

The glove will be structured in three layer:

- **First layer**: inner lining of suitable material, elastic and comfortable, to avoid direct contact between skin and rubber (latex or silicone), that would lead to sensitization and sweating of the skin.

- **Second layer**: silicone rubber, in which to integrate transducers with some techniques. The rubber allows to follow as much as possible hand movements without hampering and to measure the external forces. The silicone rubber will be added both on the palm and on the back of the hand. The main choice is Dragon Skin, thanks to its adherence and flexibility. Anyway, there is the intention to test other rubbers, such as PDMS. Subsequent mechanical tests, such as tensile and stress strength, will lead to the choice of the best product for the purposes of the project.

- **Third layer**: outer coating obtained with the same rubber selected for the first layer, with a protective function for the transducers and the circuitry, also providing greater stability to the whole structure.

3.1.1 Sensors positioning

A crucial step in the designing and the realization of the glove is the sensor disposition, that is why some disposition are been tested before taking in account the best one. In order to create the best disposition is necessary to understand better the associated

movements of the finger joints while performing elongation and flexion. Results showed that what a fiber is able to bear is not enough because the finger joints stretch around 14%. To overcome this problem there are at least three different solution, the first one is to put the sensor on the side of the joint and not on the top. This solution guarantee the elongation but the sensor is placed closer to the midline, where there is no elongation. Therefore the values of the measured elongation will ranging between the min and the max because the fiber is placed in that range. The proposed solution has also a drawback, because the wrinkles on the surface of the glove can affect the measurements. The second solution is to take the fiber and wrap it around the finger like a coil, thanks to this disposition there will be a spring effect when the hand perform the flexion and the extension. Also this solution has its own drawbacks, in this case is the stress that is caused by the wrinkles when the fingers close that will damage the optical fibers and could bring to breakage. The third solution was realized by putting the fiber in a curvilinear layout. This layout was similar to the coil's approach but was performed in a 2D structure. This disposition enables a longer elongation range.

To manufacture the sensing glove based on FBG technology it is necessary to overcome the challenge of the fiber integration. In this project is proposed to fully integrate the fiber in a flexible structure like polymers. This approach has two main advantages, the first is that integrating optical fiber in an polymeric array ensure the correct and right positioning of the sensors and the second is that guarantee also a protection of the fibers.

Here are presented some of the analyzed but not taken into account dispositions:

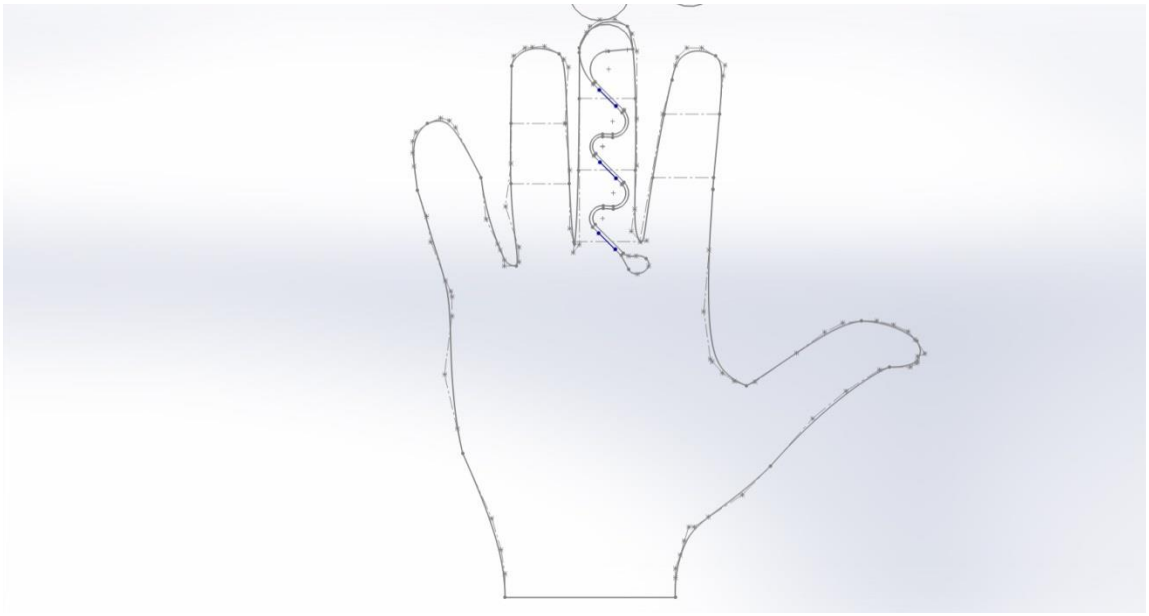

Figure 14 – Palm of the hand – Configuration 1

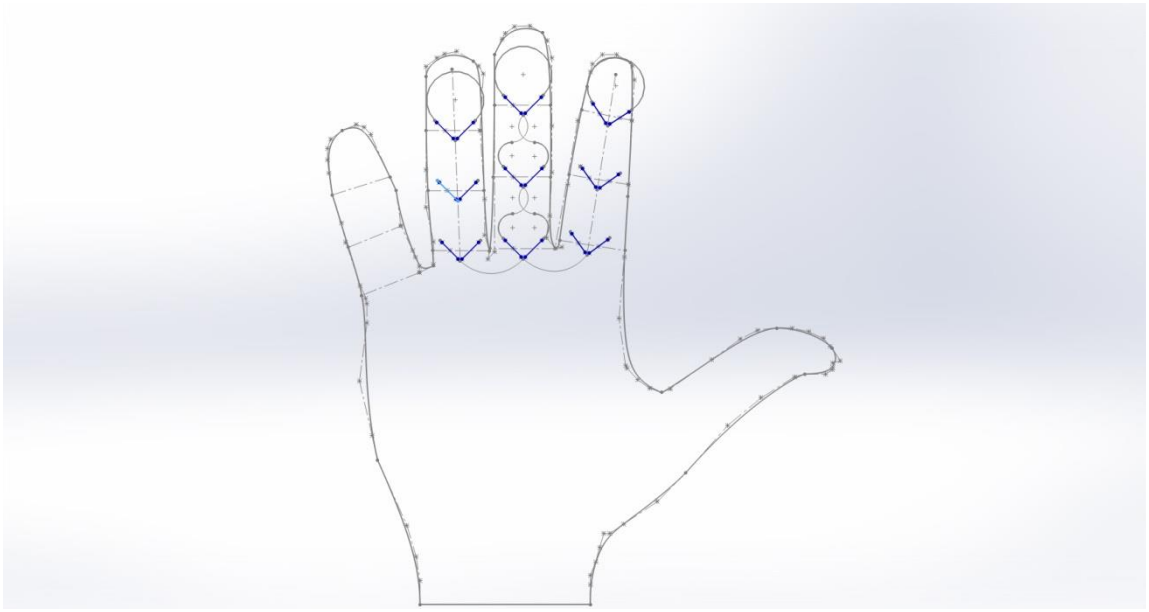

Figure 15 - Palm of the hand - Configuration 2

3.1.2 Palm of the hand

The glove will be structured with FBG transducers located in appropriate positions on the palm, so that the main forces exerted by the hand in the most frequent operations of grasping and manipulation of objects are acquired. An appropriate transducers

localization is shown in Figure 16. These should be situated on fingers for a total of 12 sensors. In this way it would be possible to acquire external forces.

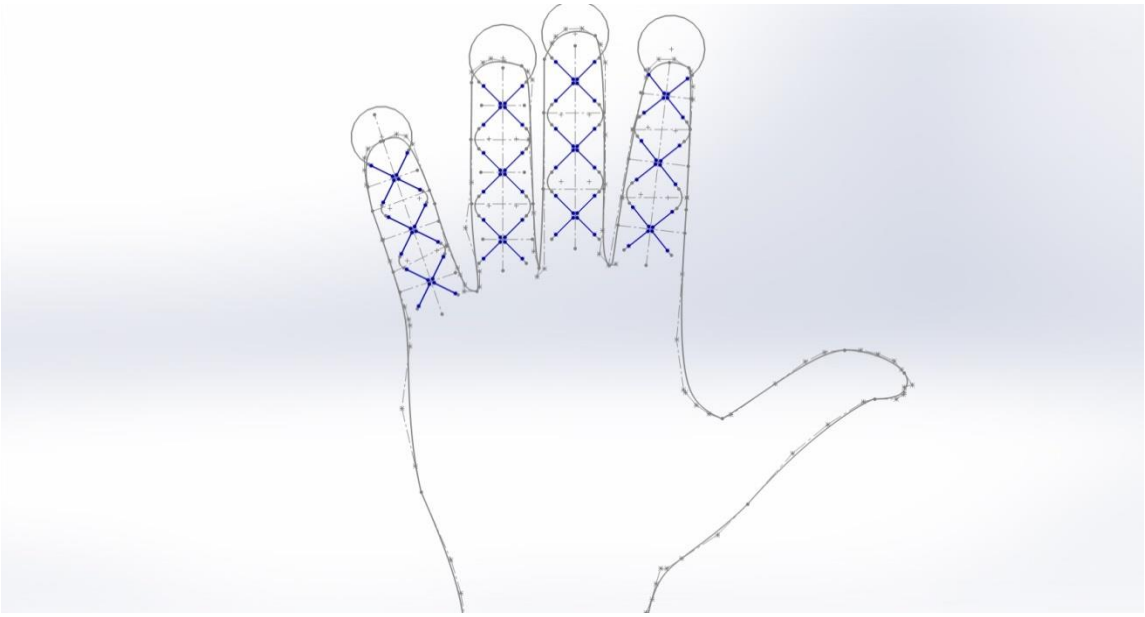

Figure 16 - Palm of the hand - Configuration 3

3.1.3 Back of the hand

The movements that have to be take in account are the flexion and the extension of the finger and also the kinematics of the hand, to ensure such requirements a sensor have to be placed over each phalanx joint. By placing a FBG sensor over each joint when the hand make a movements the FBG sensor suffer a modification in his wavelength and so is possible to make the measurements.

The human hand has 14 joints where the sensors have to be placed, but thanks to the multiplexing capability this issue require only one single fiber (Figure 17). Besides, the FBG's sensitivity enables the required spatial resolution to monitor the finger's range of movements [49].

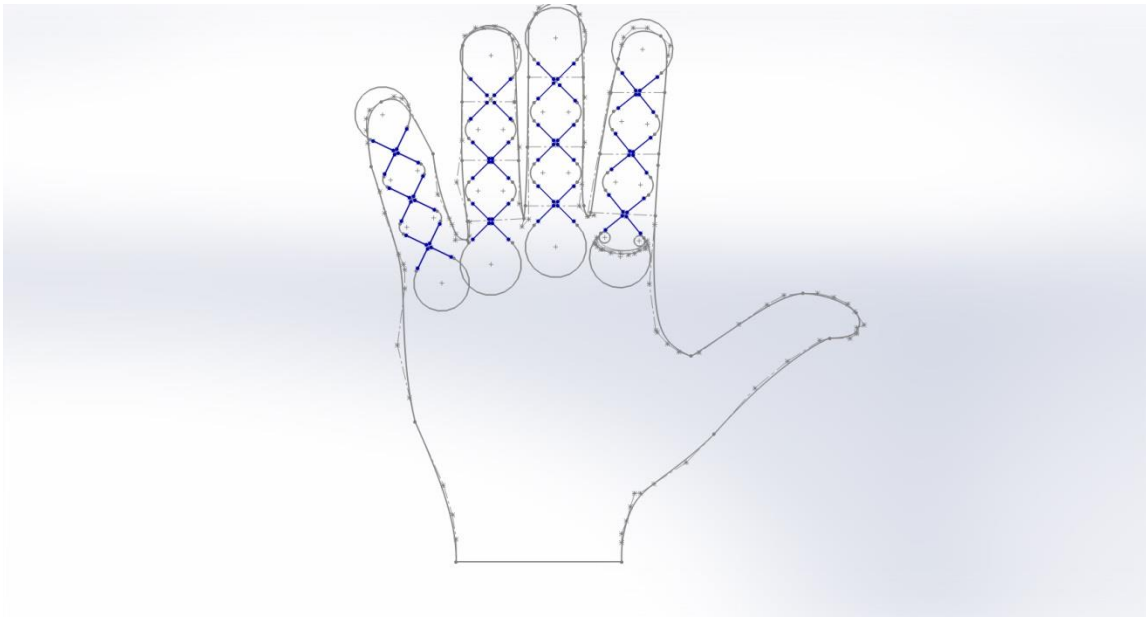

Figure 17 - Back of the hand - Configuration 3

3.2 Materials and components

A detailed analysis of the different materials needed for the device development follows below.

3.2.1 FBG Sensors

The sensors to be inserted in the glove will be made with FBG fibers. The aim is to purchase them from different providers, testing different types and finally choosing the more suitable for the project. The selected one is a fiber made by a company called FBGS [50], this is a Belgian/Germany based developer and manufacturer of high strength FBGs using draw tower technology, where the grating array is written during the drawing process of the fiber. Thanks to this process, the optical fibers integrating the gratings have some unique properties like high quality and affordable price. The fields of application of this kind of sensor are several such as medical, transport, civil and R&D.

The purchased fibers is called DTG (draw tower gratings), this is a fiber used for measurement of temperature and strain, which may be attached to a textile or embedded in it. There are two possible diameters for this fiber 80 and 125 µm. Draw Tower Gratings (DTG®s) are produced using a process that combines the drawing of the

optical fiber with the writing of the grating. The aforementioned process of writing the gratings and at the same time drawing the fiber realized high strength FBG chains. The fiber are then coated with a special polymer called ORMOCER after the writing of the gratings. This kind of fiber have some unique characteristics that makes them very suitable for the sensing glove.

Extremely high mechanical strength

The comparison of normal optical fibers and FBG show that FBGs have extremely high mechanical strength. This characteristic is tested by applying increasing tensile stress to the samples until the breakage of the fiber

Direct fixation

As stated before the coating of the optical fiber is ORMOCER, which is an organic modified ceramic. The main characteristics is the optimal adhesion to the fiber, which makes the FBGs applicable in a direct way to the structures, facilitating the installation process and increasing the reliability

Spliceless Arrays

In a single fiber it is possible to have a high numbers of elements. The only constrain is that the band occupied by an FBG is not overlap by another FBG. Figure 18 shows the spectrum of an array of 80 FBGs on a single fiber, all with different wavelength.

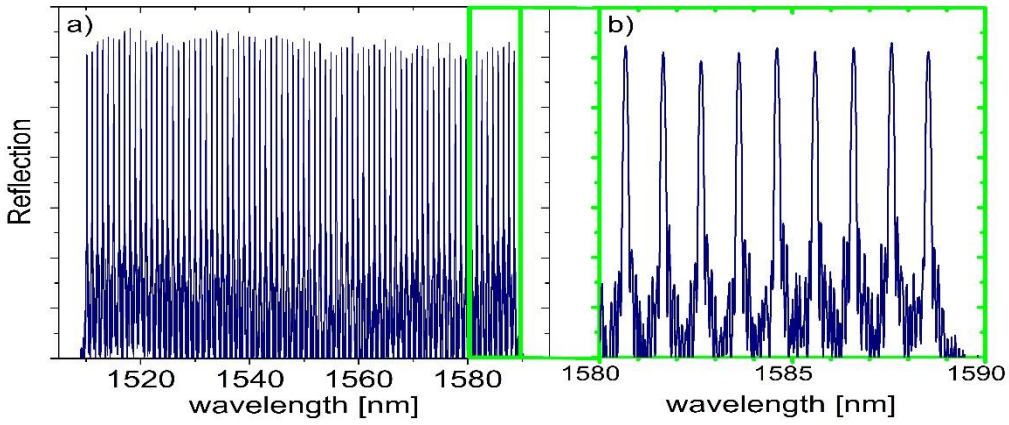

Figure 18 – Wavelength diagram [50]

Uniform coverage coating

An important task is to have a uniform coating over the full length of the fiber, this is possible with this procedure where none stripping or recoating process is necessary.

High operating temperature range

These optical fibers are able to withstand a wide range of temperature, from -180 to +200°C, the operating temperature is limit by the coating with ORMOCER material

Low bending loss

In smart textile integrating optical fibers it may happen that there are configuration with low bending radii, is very important to not have a relevant attenuation effect caused by this bend.

High repeatability

Repeatability is guarantee thanks to the control of every parameter, this is possible because to produce the FBGs is used an automated production process.

Relatively low cost

The FBGs are realized using a full automatic production process, so in case of high volume orders the price of the fibers became smaller.

Reflectivity is one of the most vital parameters when analyzing the optical fibers with FBGs, generally a silica written FBG has a reflectivity of >90%. Compared to this one the reflectivity of DTG is lower, about 25% (typical value range around 20%). This reflectivity seems to be too low and could cause problems in the measurements set-up, but in practice, for almost all the interrogation units there are no kind of problem both for static and for dynamic measurements

Static measurements devices are characterized by a large dynamic range (>30dB). In the figure below are showed three different type of FBGs, the first is a high reflective FBG with values above 90%, then the second, which is the DTG with lower reflectivity, around 25% and at the end a FBG with very low reflectivity, about 4%. What appear evident is that even the 4% reflectivity FBG, thanks to the dynamic range of the device, can be

measured with a Signal to Noise ratio of 13 dB, which is above the safe detection od 10 dB

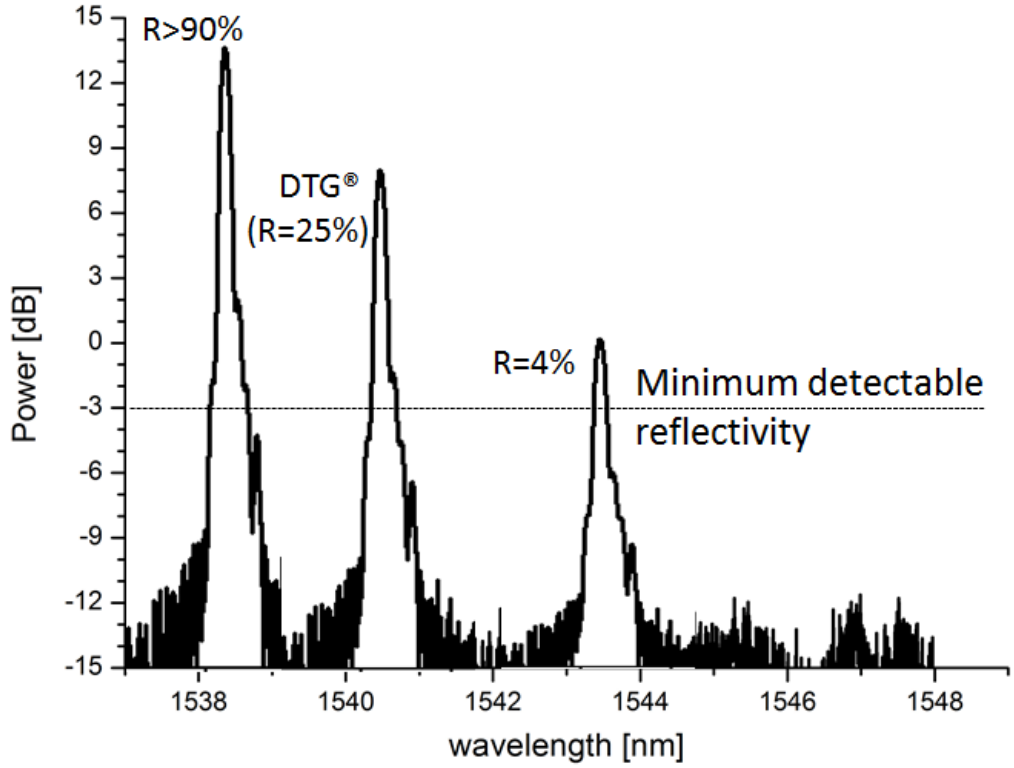

Figure 19 - Static measurement device [50]

The question for dynamic measurement devices is more complicated because generally they have a lower dynamic range (<25 dB), but these systems can be modified by changing the laser light power or the integration time. The first for tunable laser based systems the second for photodiode. After the optimization of the Signal to Noise ratio also the low reflectivity of DTG can be compensated with the increase of one of these two parameters. In the next figure (Figure 20) is showed a comparison between three different spectrum, the first is the spectrum of a standard DTG with reflectivity around 25% , the second is the spectrum of a high reflectivity FBG, about 90% and the last is a FBG with very low reflectivity, about 3%. All the measurements were taken with the same interrogation unit, the micron optics SM130 device. This system is a dynamic one and is based on a tunable laser. For each of the showed grating the power of the laser was optimized by adjusting the gain in the software. For high values of gain setting there were higher optical power supplied to the fiber in order to detect the wavelength of the FBG. As it is showed in the figure, for high reflectivity FBGs, the gain had to be set to 1 dB to

have an acceptable Signal to Noise ratio. For higher gain values the system would be saturated and not able to detect the FBGs. 11.5 dB is the optimal gain for a DTG, furthermore in this case high gain values lead to a saturation of the detectors and for that makes the readings not usable. The maximum gain of the device is 20 dB so it appear evident that there is still the possibility to add additional losses that will be introduced by the network such as too long fibers, bad connectors, optical splitter. Eventually also the low reflectivity FBG could be easily measured using a gain of about 18.5 dB

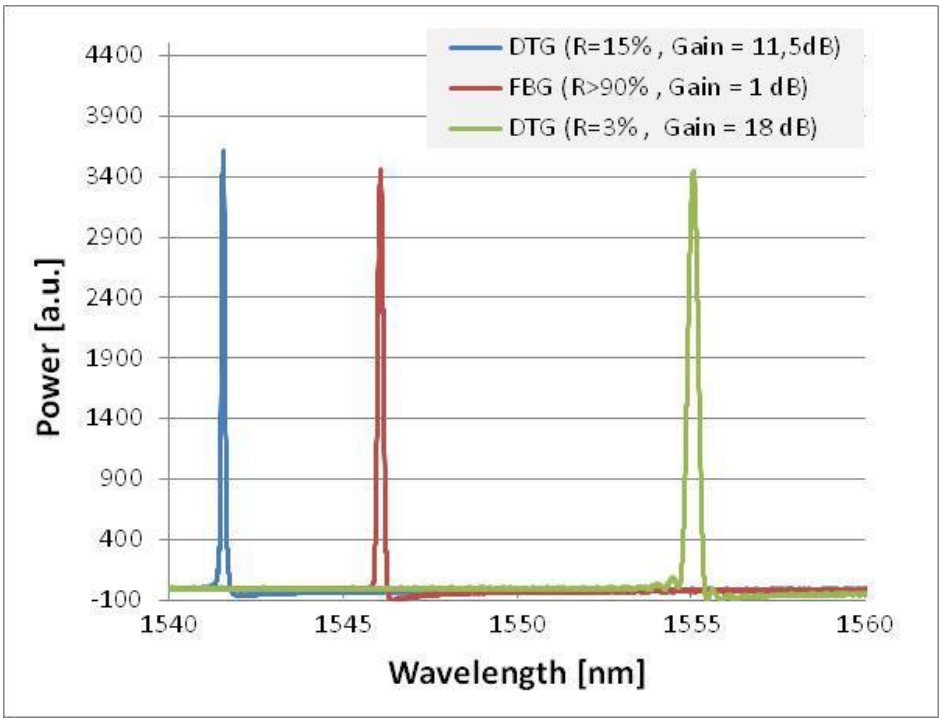

Figure 20 - Dynamic measurements device [50]

As stated in the beginning an optical fiber integrating FBGs is sensitive to both temperature (T) and strain (ε) changes, so is possible to write the following equation:

$$ln\frac{\lambda}{\lambda_0} = S_\varepsilon \Delta\varepsilon + S_T \Delta T \qquad (1)$$

Where λ is the FBG-wavelength; λ_0 the wavelength at an arbitrary reference strain ε_0 and a reference temperature T_0; S_ε the strain sensitivity or gage factor; S_T the temperature sensitivity; $\Delta\varepsilon = \varepsilon - \varepsilon_0$ the strain change with respect to the reference strain and $\Delta T = T - T_0$ the temperature shift with respect to the reference temperature.

The equation (1) refers only to FBG that are not fixed to any kind of structure. When FBG are not free of holds the equation should be adjusted due to the thermal expansion of the structure where is attached the sensor. When there is a linear expansion coefficient α_t, then the thermal expansion of the structure is given by α_t. ΔT. When instead there is an expansion that exceed the thermal expansion of the fiber glass, which is α_f ΔT, there is an extra strain that the structure add to the fiber, this added value is equal to (α_t - α_f) ΔT. Knowing that only the excess expansion will be transferred into the strain, we have to take in account the differences of the various thermal expansion coefficients. This strain gives an additional wavelength shift corresponding to S_ε (α_t - α_f) ΔT. The modified formula thus is given by:

$$ln\frac{\lambda}{\lambda_0} = S_\varepsilon \Delta\varepsilon + [S_T + (\alpha_t - \alpha_f)S_\varepsilon]\Delta T \qquad (2)$$

FBGs can be used both for measurements of strain and temperature, but this characteristics can also be a drawback. When it is necessary an accurate measurement of strain, the presence of temperature changes is negative, so this require gratings that have to work in parallel. The first FBG used has to be sensitive to both temperature and strain but the second has to be isolated from the possible strains in order to be able to measure only the temperature. Therefore, the cross-sensitivity is not such a big deal, but of course some adjustments have to be considered. This problem was underline also by some research, in 2012, Witt et all made the measures at room temperature but after 3 hours testing there was a drift of about 15 pm caused by a changing of the temperature in the laboratory. The FBG has a temperature sensitivity of about 10 pm/K. Although the need of this temperature compensation there are some paper in which the strain-thermal cross sensitivity can be avoided. Liu et al in 2006 saw that in his FBG sensor within a temperature range, the reflection wavelength of the FBG sensor shifts from 1558 to 1558,6 nm. Since all sections of the FBG experience the same temperature fluctuation, all the relative changes suffered by the sensors were more or less the same. Another interesting study is the one of Grillet et al, in this case no correction of the measured wavelength shift of the FBG was take in account because during the tests the room temperature was quite stable.

The DTG's in reduced cladding diameters are written in an 80 µm glass fiber. These DTG's offer some interesting properties in comparison with the standard 125 µm DTG fibers. Because the fiber is thinner: 1) when the fiber is embedded in textiles it is less invasive and annoying, 2) this fiber is more elastic so the main advantage is that can be successfully used in those application that require small bending radius, 3) in order to strain the fiber the required force is lower so this characteristic make this fiber excellent for acoustic sensors or hydrophones. Both those fibers currently offered the 1550 nm windows and is drawn with an Ormocer coating.

The FBG fibers don't have to reach the breakage and so to prevent this episode, the strain should be as low as possible in respect to the application. In Figure 21, it is possible to see that fibers with lower diameters (80 µm) are more indicated to withstand low bending radius.

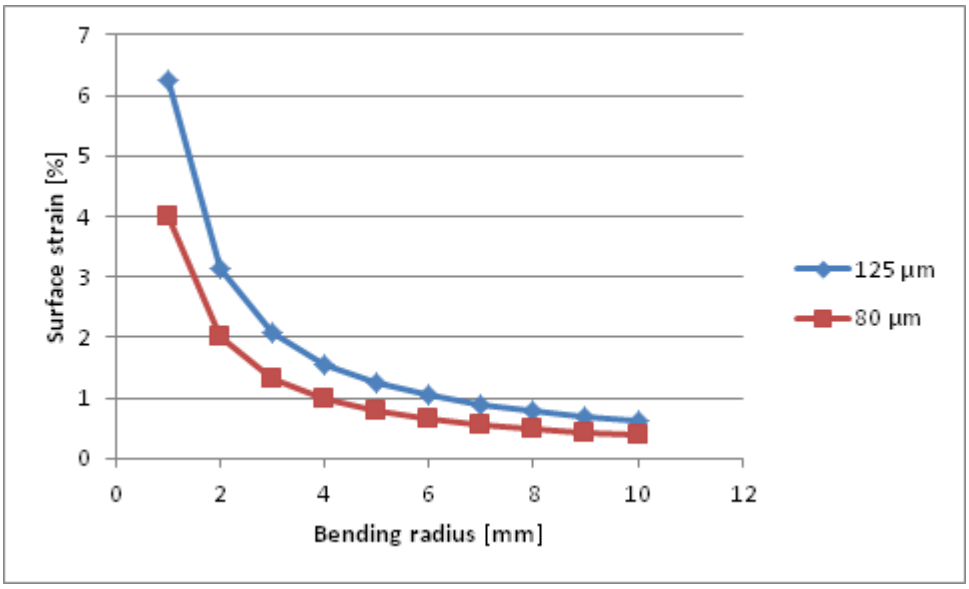

Figure 21 - Surface strain as function of the bending radius for a fiber of 80 and 125 µm [50]

What is the real limiting factor for the small bending radius is the bending induced strain at the fiber glass. Bending strain in the fiber comes out when an optical fiber is coiled, in fact for large strain values it brings to fiber damage or even fiber breakage. The maximum value of strain caused by bending is at the fiber surface. To calculate this strain is possible to consider the strain as a function of the fiber diameter and of the bending radius. In the figure above is showed the surface strain as function of the bending radius for an 80

µm diameter fiber and 125 µm diameter fiber. Generally thanks to his properties, the DTG sensor have very low losses due to the bending, in the Table below are illustrated some measurements taken in presence of a bending radius. As can be seen the attenuation per winding for millimeter sized radii is less than one dB.

Radius [mm]	Windings	λ [nm]	Total attenuation [dB]	Attenuation / winding [dB]
3.75	20	1550	0	0
2.5	20		0.1	0.005
2	5		0.75	0.15

3.2.1.1 Datasheet 80 and 125 µm

Draw Tower Gratings in Low Bend Loss fiber - 125µm

Parameter	DTG – A3A4
Reflectivity (gratings about 8 mm)	>15%
FWHM (gratings about 8 mm)	100pm
Centre wavelength	1510 to 1590nm
Wavelength accuracy	≤0,5nm
Relative wavelength accuracy	≤0,3nm
Side Lobe Suppression (SLS)	≥ 10dB
DTG® length	1 to 10mm /8mm (typical)
Attenuation	8,6 dB/km
MFD (Mode Field Diameter)	6µm
NA (Numerical Aperture)	0,26
Cladding diameter	125µm ± 1µm
Coating type	ORMOCER
Coated fiber diameter	195µm
Tensile load at break	>50N

Temperature sensitivity-formula: Δλ/(λ x ΔT)	$6{,}5K^{-1}$x 10^{-6}
Strain sensitivity1-formula: Δλ/(λ x Δε)	$7{,}8\mu\varepsilon^{-1}$ x 10^{-7}
Operational temperature range	-180°C → 200°C

Draw Tower Gratings in Low Bend Loss fiber - 80µm

Parameter	DTG – A2A3
Reflectivity (gratings about 8 mm)	>15%
FWHM (gratings about 8 mm)	100pm
Centre wavelength	1510 to 1590nm
Wavelength accuracy	≤0,5nm
Relative wavelength accuracy	≤0,3nm
Side Lobe Suppression (SLS)	10dB (typical)
DTG® length	1 to 10mm /8mm (typical)
Attenuation	8,6 dB/km
(MFD) Mode Field Diameter	6µm
Cladding diameter	80µm ± 1µm
Coating type	ORMOCER
Coated fiber diameter	115µm
Tensile load at break	>20N
Temperature sensitivity-formula: Δλ/(λ x ΔT)	$6{,}5K^{-1}$x 10^{-6}
Strain sensitivity1-formula: Δλ/(λ x Δε)	$7{,}8\mu\varepsilon^{-1}$ x 10^{-7}
Operational temperature range	-180°C → 200°C

3.2.1.2 Wavelength and spatial configuration

One of the interesting advantage of the FBG is the possibility to reduce the cabling requirements and the possibility to have an easy installation. Thanks to the multiplexing techniques the FBG sensors can simultaneously read large numbers of sensors on a single

fiber. It is possible to put more than one gratings (generally up to 80) in a single fiber, however there is a limit due to the overlap of the wavelengths. Every single FBG has is reference wavelength (i.e. 1500 nm), when a deformation is applied there is as effect a wavelength variation and this variation have to be smaller than the reference wavelength of the next FBG. When there is an overlap of one of the two FBG, one signal is lost.

The spatial configuration is an important task due to the integration of the fiber on the glove. To make the right configuration the gratings have to follow a specific sequence and distance.

In order to be able to finalize the purchase order it was necessary to decide the wavelength and the spatial configuration. The issue was to combine the specification of our project with the configuration possibilities given by FBGS company. As we see in Figure 22 there are several possibilities, we have chosen the one with flexible spacing and short distance.

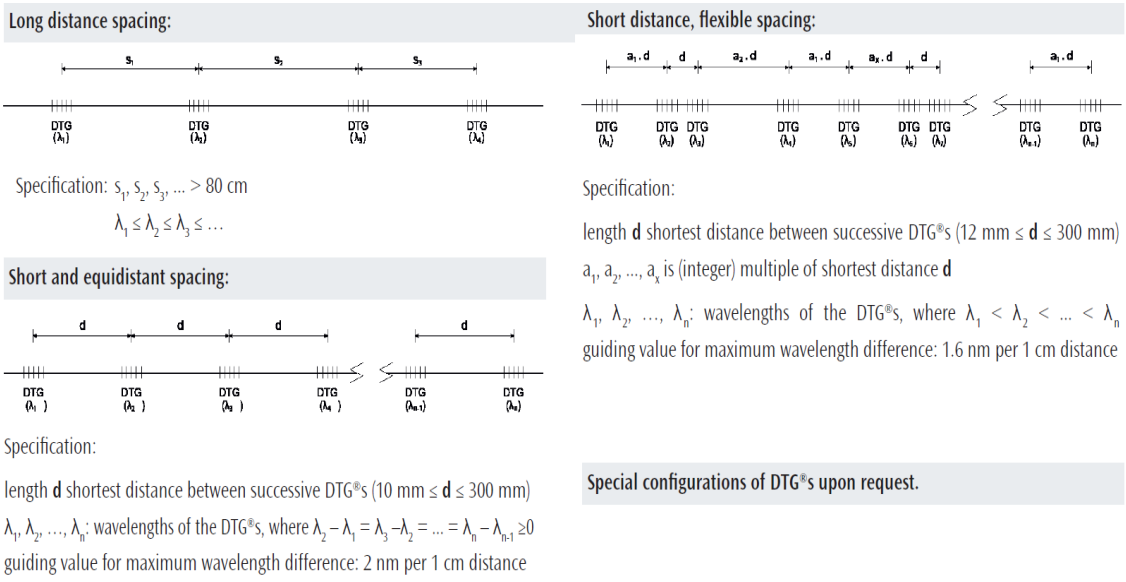

Figure 22 - Configuration possibilities [50]

So according to those issues we have found our wavelength and spatial configuration, (Figure 23 and Figure 24). The wavelength is expressed in nanometers and the spatial configuration in millimeters.

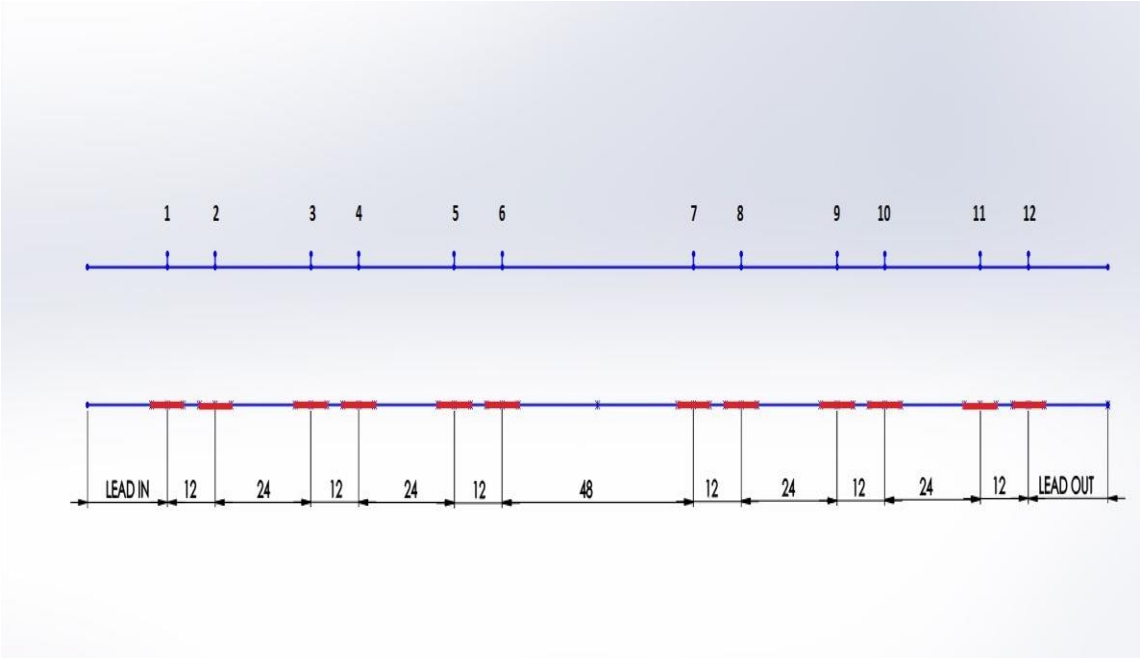

Figure 23 - Wavelength and spatial configuration, the FBGs are marked in red

#	Wavelength (nm)	Distance (mm)	Position
1	1532,9	0	Cross 1
2	1534,8	12	Cross 1
3	1538,6	36	Cross 2
4	1540,5	48	Cross 2
5	1544,3	72	Cross 3
6	1546,2	84	Cross 3
7	1553,8	132	Cross 3
8	1555,7	144	Cross 3
9	1559,5	168	Cross 2
10	1561,4	180	Cross 2
11	1565,2	204	Cross 1
12	1567,1	216	Cross 1

Figure 24 - Table of Wavelength and Spatial configuration

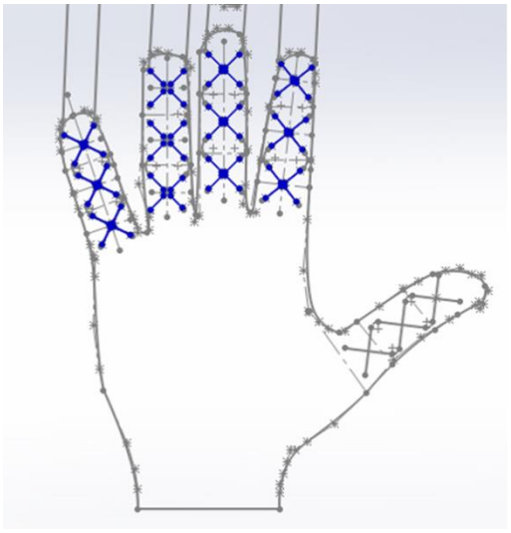

Figure 25 - Sensor disposition

3.2.2 Interrogation unit

To obtain the measurements from an FBG sensor, this have to be illuminated by a light source. What is measured is the reflected wavelength and the change that occurs when there is a strain. Shifts in the Bragg wavelength will then be monitored.

Pilot prototypes will be developed using optical sensing interrogator tests in order to make fast, simultaneous, measurements of several fiber-optic temperature and strain sensors. This interrogators will not be portable and suitable for the project but will be used in order to simplify preliminary tests.

3.2.2.1 Si425 Optical Sensing Interrogator

A possible interrogator will be the “si425 Optical Sensing Interrogator” (Figure 26) [51].

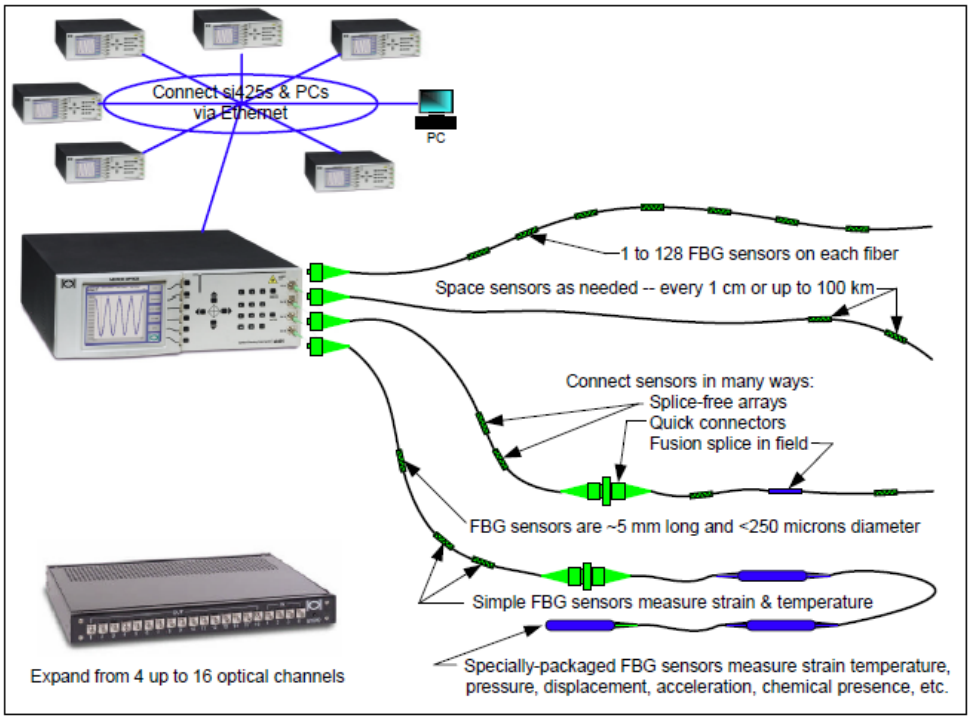

Figure 26 – Optical interrogator [51]

Benefits

Calibration - This interrogation unit do not need a calibration phase because the wavelength is automatically calibrated on each scan

Robust Operation – this device is design and produce in order to resist and survives in several and harsh environments.

Huge FBG Sensor Capacity – this machine has extraordinary ability to monitor a very high number of Bragg grating sensors. Users have great flexibility in the design of their own sensing system because the si425 have 80nm of wavelength range per channel and up to 16 optical channels.

Fast Peak Detection – generally the measurements are taken at 250 Hz, this is possible thanks to the on board peak detection circuitry that is very efficient and fast.

Rack Mountable – to be able to resist to vibration, shocks and wide temperature changes the device is given in a protective enclosure

Verifiable Performance – the performance of this device are the same that are stated on internet, there are no surprises while using it in many applications.

Modular Design – there are at least three possible configurations, customers may design their device in the way they want. For example some si425 instruments have a display in the front panel. For data analysis the devices are linked to the PC via Ethernet.

The si425 is offered in three standard models. Custom configurations allow optimization of unit costs and feature sets for volume customers. Some si425 instruments have a built-in display and front panel controls. All use Ethernet to network to external PCs for additional data analyses.

3.2.2.2 I-MON High Speed

In a second phase we will use a portable system in order to be more suitable with the project. An example of portable interrogator can be the I-MON 256 High Speed (Figure 27): this device is able to scan up to 35 kHz for full spectrum monitoring of all the FBG sensors. The measurements of a large number of FBG is provided by the combination of a high resolution monitor and a high spectrometer resolution. This interrogation monitor offers full spectrum monitoring of FBG sensors at line scan rates up to 35 kHz. A high spectrometer resolution combined with a broad wavelength range provides high-resolution interrogation monitors, allowing measurement of a large number of FBG sensors.

To enable the plug and play operation for FBG sensing sensors, the interrogation unit provide a data acquisition software and an interface software [52].

Figure 27 – I-MON High Speed [52]

This device showed in the figure above its provided with a LabVIEW source code with an Evaluation software and with the DLL and the drivers for OEM integration.

The main interesting characteristics of the evaluation software is the possibility to analyze in an easy and fast way the performance of the I-MON. this interrogation unit will have miniaturized dimension: 124x94x59 mm, according to the project need of short use.

3.2.3 Development of the tactile sensor array integrating FBG

This part reports about the development of the tactile sensor array integrating FBG transducers for hand biomechanical measurements. The fiber bragg gratings elements are embedded in a thin polymeric sheet in order to make this sensor, which is a sensing pad with a very low thickness of 1 mm.

The fabricated pad sensor will be added in the glove and will be in further studies combined with a portable interrogation unit. For the purpose of the project, a high physical dimension device is not suitable with the portability of the complete sensing system.

The 2D surface sensing is realized by embedding the optical fiber with the FBG elements in this 2D structure, as shown in Figure 28. The used polymer is called Dragon Skin, the properties of this polymer are suitable with the sensing application since it is flexible, stretchable and is possible to control the viscosity and the harness. Thanks to his characteristics this sensing pad is able to measure several mechanical quantities like deformation, strain and pressure along the whole surface. Furthermore, the pad may be embedded, attached or wrapper around the glove.

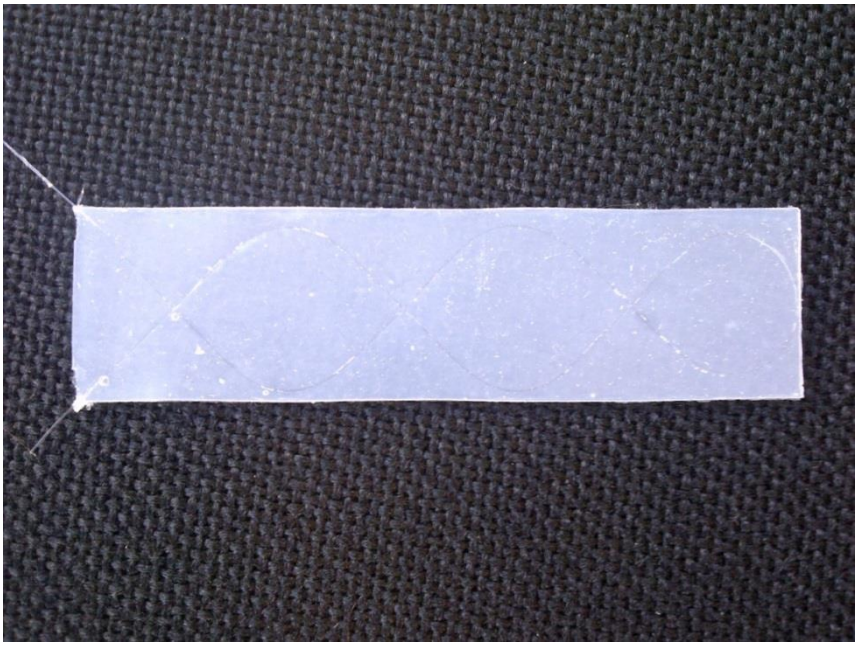

Figure 28 – Tactile sensor array integrating FBG transducers for hand biomechanical measurements

For the fabrication of the sensing pad we used plastics and metal molds. To realize the plastic piece Figure 29, which is the core of the complete mold it has been used 3D printer.

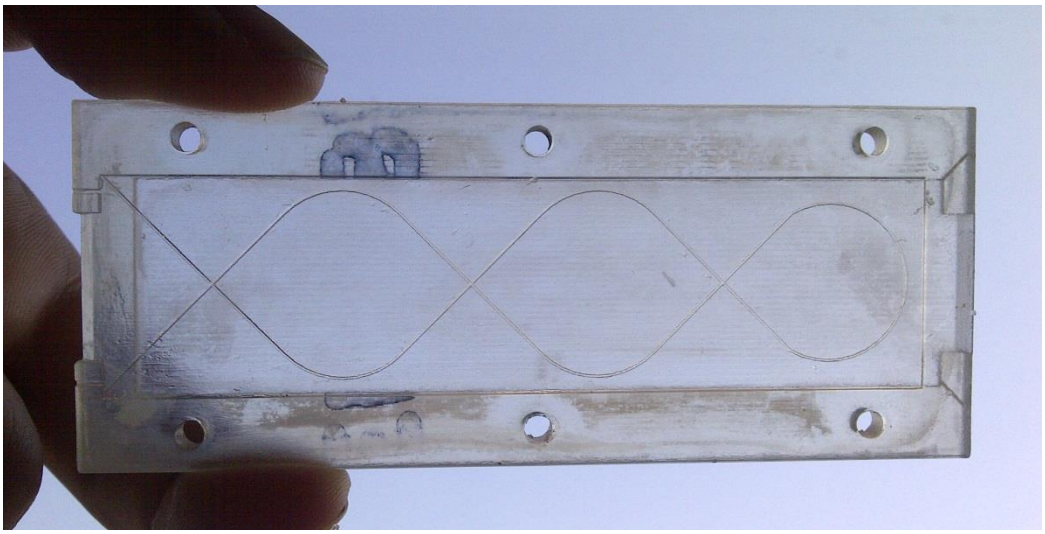

Figure 29 – Central part of the mold

A 3D printer is a machine able to make three-dimensional object. The realization of the different objects begin with an additive process in which successive layers of the selected

material are laid down under the control of the computer. The interesting thing is that the created objects can be of almost any geometry and shape, the production of this 3D model begin with the help of the computer. Thanks to CAD (computer aided design) is possible to create the models that would then realize the 3D object. In this project the software used to make the CAD was SolidWorks.

This plastic part is 3 mm thick and has two faces: on one side (Figure 30), the front one, there is a cut extrusion of 0,5 mm and inside this there is also an extrusion of 250 µm that follow the future optical fiber disposition. On the other side (Figure 31) there is just a cut extrusion of 1 mm.

The metal parts were more easily to make and were thick 4 mm, Figure 32. This parts has the function of coverage and stability to the central part. In Figure 33, we can see the complete mold.

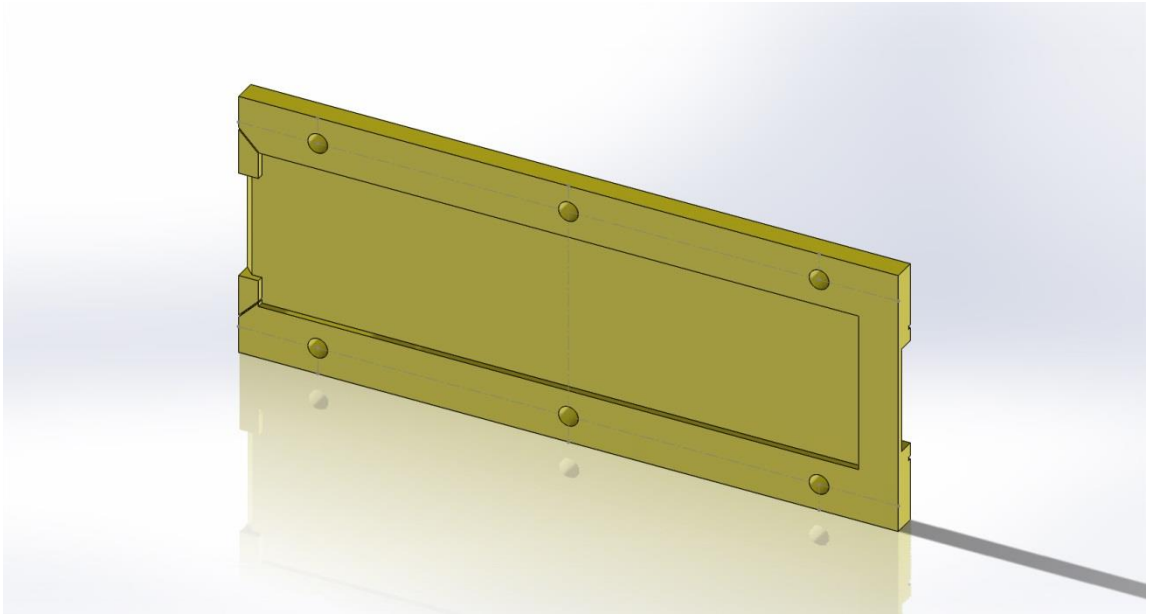

Figure 30 - Back of the mold

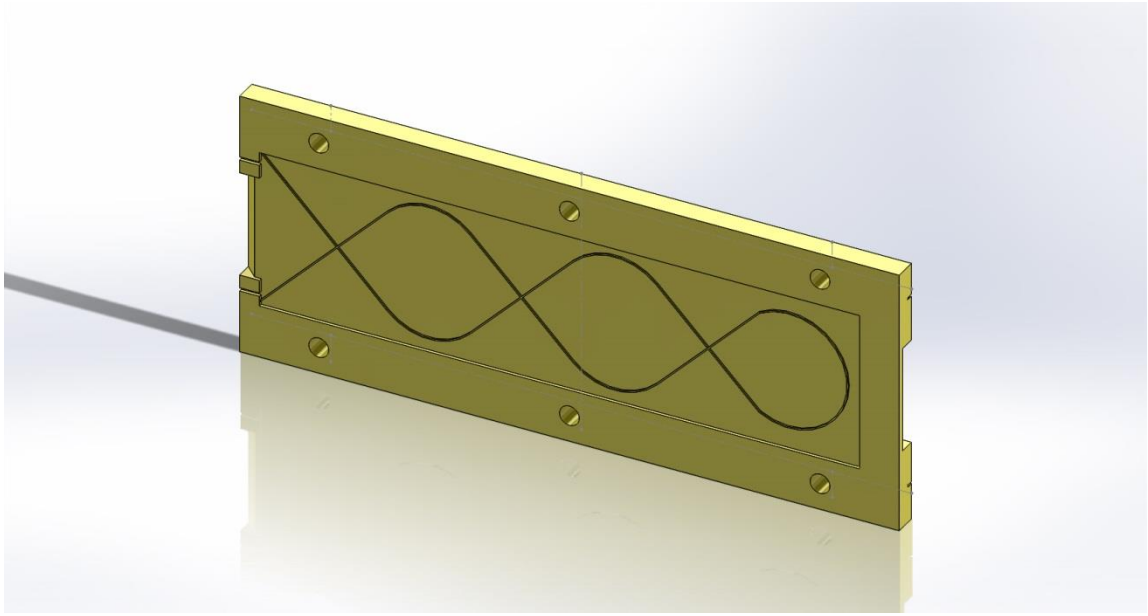

Figure 31 - Front of the mold

Figure 32 - Metal parts

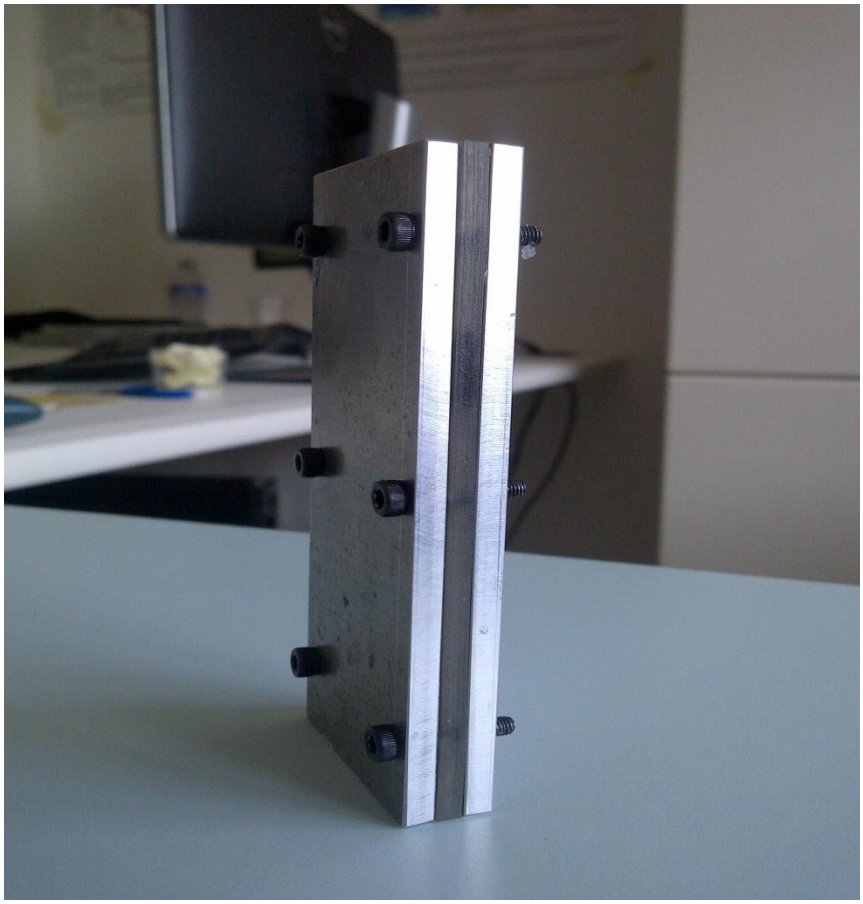

Figure 33 - Complete mold

The realization of the pressure tactile sensor is divided in three parts:

- **First Part**: Realization of a layer of 0,5 mm of Dragon Skin with a groove that follow a specific design. The extrusion in the central plastic part is the same of the future disposition of the optical fiber. So after completing this first part, we realized a thin layer of polymer with this groove where we can put the optical fiber
- **Second Part**: Insertion of the optical fiber in the groove with the help of silicon glue
- **Third Part**: Realization of a layer of 1 mm of Dragon Skin with the optical fiber inserted in the middle. After completing the second part we have a layer of 0,5 mm with the optical fiber inserted on the top. Next we put the sensor on the cut

extrusion of 1mm and we cast above silicon to cover and fill the cut extrusion. At the end we realize the tactile sensor integrating FBG with a minimal thickness of 1mm and the fiber in the middle.

The casting of silicon also followed a specify procedure which is describe here after:

In a plastic glass is putted the Dragon Skin and the silicon thinner, after degassing for some cycles the mixture, the silicon was inserted in the oven at 80 degrees for more than one hour. At the end the mold was taken and separated in order to extract the tactile sensor integrating FBG.

4 Experimental evaluation of the developed sensorized glove

This section analyses the experimental phase. This work shows the characterization of a tactile sensor array integrating FBG transducers for hand biomechanical measurements. The analysis of the response of the array while varying the probing location was carried out to assess the capability of the sensor to detect and discriminate loads in generalized conditions. The FBG-based array was experimentally evaluated with a testing machine (Instron, 5900 Series) to obtain the relationship between the applied Force and the wavelength variation. The sensor response was evaluated with different indentation locations. Some metrological properties, such as repeatability and accuracy, were estimated. The sensor was designed and developed at the BioRobotics Institute of Sant'Anna while the measurements were taken at Campus Biomedico of Rome.

4.1 Experimental setup for applying mechanical stimuli to the sensors

Instron [53] has developed many of the significant progress in the materials testing industry since being founded in 1946 by two research scientists. With investment in research and development, the Instron team have produced a number of materials testing innovations – from the first strain gauge load cell to all-electric dynamic systems to video exstensometry. Their ambition to continually innovate and develop new products is driven by the engineering and technical expertise designing systems and accessories with their core philosophy of data integrity, safety and protection of investment in mind.

Today, Instron offers some of the highest-quality and most accurate testing equipment on the market with product lines that cover a wide range of mechanical testing needs from tension testing to complex service life simulation. The goal is to provide the customers with the best ownership experience by delivering the highest quality products, accessories, and software that offer accurate and reliable test results, time saving, and the flexibility that is necessary for the industry's ever changing demands. For static testing in a tensile the most used devices are the electromechanical one, they can also perform pull tests and other additional tests such as tension, shear, peel, flexure, compression and bend test. Normally the capacity of these systems goes from low forces

of about 0.5 kN to high capacity of about 600 kN test frames. Instron have two series that fulfills these requirements, the 5900 Series and the 3300 Series. The first one is generally used in application that need advanced testing requirements that are typical found in development laboratories, while the second is a more affordable line used in Quality Control.

In our experimental analysis we used the Instron 5900 Series (Figure 34). This Series of mechanical testing systems offer some unique properties such as high accuracy and reliability. The data acquisition rate can be estimated to a value of 2,500 points per second, which is very fast, and the accuracy of the measurements are +/- 0.5% of reading down to 1/100 of load cell capacity. The 5900 Series is an optimal device and his application may range in several application, the most common uses are for compression, peel, tear, bend and tensile. The most important characteristic is the reliability of the device.

Figure 34 - Instron Setup [53]

The primary reason of excellent characteristics of this device is the attention to every single element of the system, which is demonstrate by the high accuracy, high repeatability and high reproducibility in terms of results. Moreover, the process of

recognition and calibration of load and strain transducers is automatic. Thanks to preloaded ballscrew, the guidance columns and a god drive system, the alignment and the frame stiffness is guarantee. In several application are necessary a range of additional accessories to meet the requirements of the projects, these are provided with the device and include: plastic, textiles, biomedical stuff, elastomer, and components. To use in a properly way the Instron, an outstanding interface is necessary and have to be easy to use and simple to learn. Bluehill is the designed Software that meet the demands of a wide range of applications, this software provides all the capabilities you need to handle.

In just two steps the test may be started and then what concern the control, the data acquisition, the plotting, the calculation and the reporting are completely automatic.

A cylindrical probe made with a 3D printer, with external diameter of 5 mm (surface of 16 mm^2), was used to apply deformation to the surface of the array. The material testing machine described above (Figure) was suitable to apply compression to the sensor surface. The Instron was used to move the indenter along the z-axis with constant speed of 0,1 $mm \cdot s^{-1}$, and the compression force was measured with sampling frequency of 10 Hz. the measurement range started from 1N up to 3N. Two translational stages (PT1, Thorlabs, with differential micrometer drive 150-811 ST) were used to translate the sensor along two perpendicular directions, x and y axes, with the aim to accurately control the position of the indenter above the desired surface coordinates (maximum displacement of 2,5 cm). The change of wavelength experienced by the FBGs during the compression tests was measured by means of an optical spectrum analyzer (OSA, optical Sensing Interrogator, sm125, Micron Optics, resolution of 1 pm) and acquired by a graphical user interface. The software used to obtain the data acquired at a frequency of 250 Hz, while the frequency of the Instron was 10 Hz. So in the post processing it was necessary to fix this two value in order to be able to work with vector of the same length and to plot with MatLab. During the indentation experiments the probe was applied in 12 selected sites of the sensor surface (Figure 35) with the aim to retrieve a relationship between the force applied to the sensor surface and the wavelength experienced by the FBG. Each experiment was repeated 2 times per each indentation site, thus obtaining a dataset with 24 sessions.

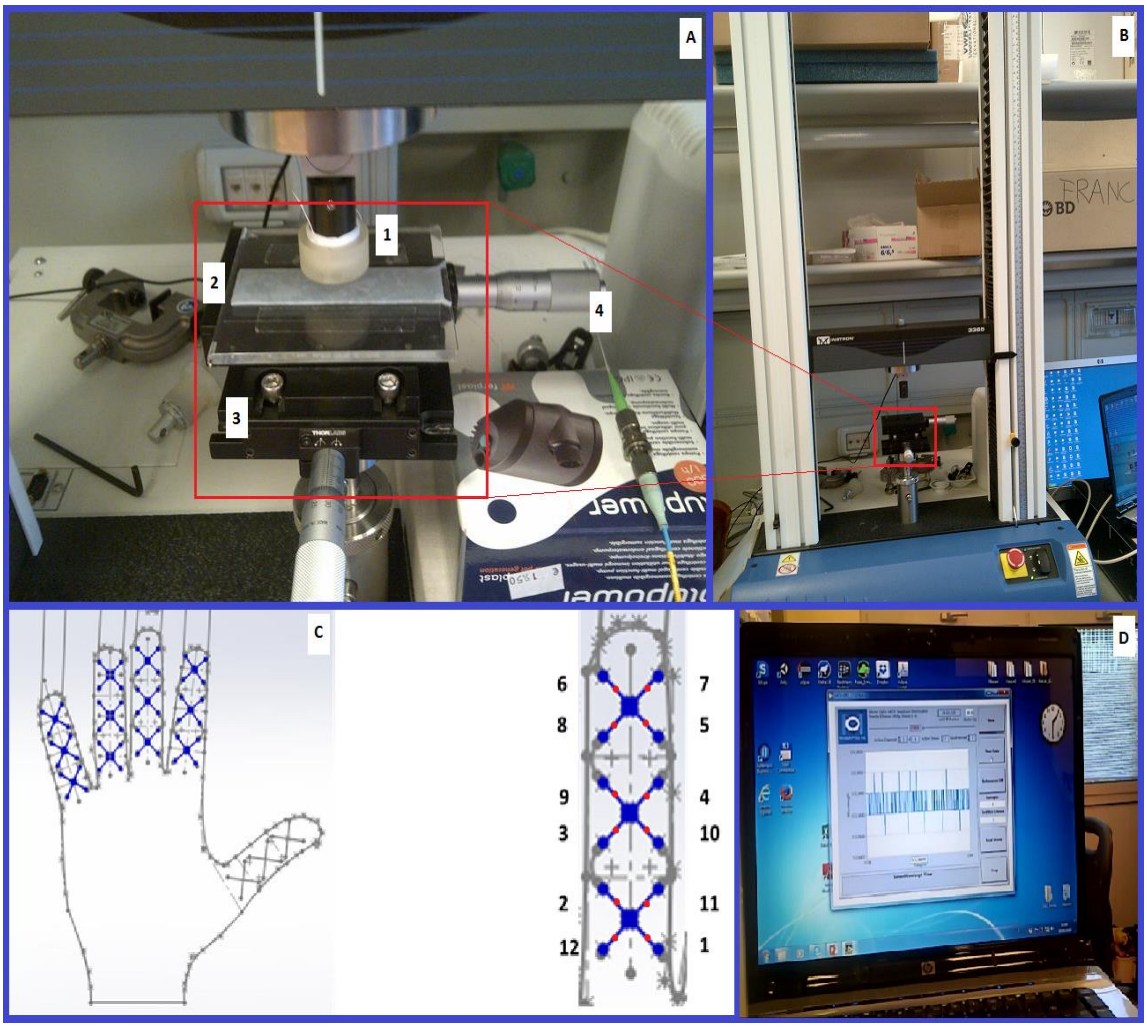

Figure 35 – Experimental Setup

(**A**) Experimental set up including: 1) the cylindrical indenter, 2) sensor array integrating FBG, 3) the Newport optical table and 4) the two translational stages. (**B**) Material testing machine. (**C**) Schematic of FBG sensor array with detail of indenter position, in correspondence of the red circles. (**D**) PC with the software to collect data

4.2 Data analysis methods and experimental results

The indentation force F was tracked by the FBGs via a coherent modulation of the wavelength registered by the OSA (Figure 36). Such modulation was monotonic and highly repeatable (Figure 37). The modulation of Bragg wavelength was dependent of

the applied force on the FBG sensor: the more the applied force, the more was the wavelength variation. In Figure 38 is show the change of Bragg wavelength when a force of 3N is applied on the sensor number 3 in direct comparison with the other 3 FBG of the indicated cross. We can see that the behavior of the 3 adjacent sensors is negligible in comparison with the sensor where is applied the force.

In order to elaborate the results, a code in MatLab has been written. With the function polyfit it was possible to make the linear regression and to fit the curves to a line. The fixed curves were with very good approximation defined by the lines (the error fit was very little, almost negligible). From these results, it was also possible to examine the sensitivity of the system thanks to the angular coefficient. In Figure 42 and 44 are showed the result of this quantitative analysis, from this dates it can be see that wavelength variation and force have a linear variation,

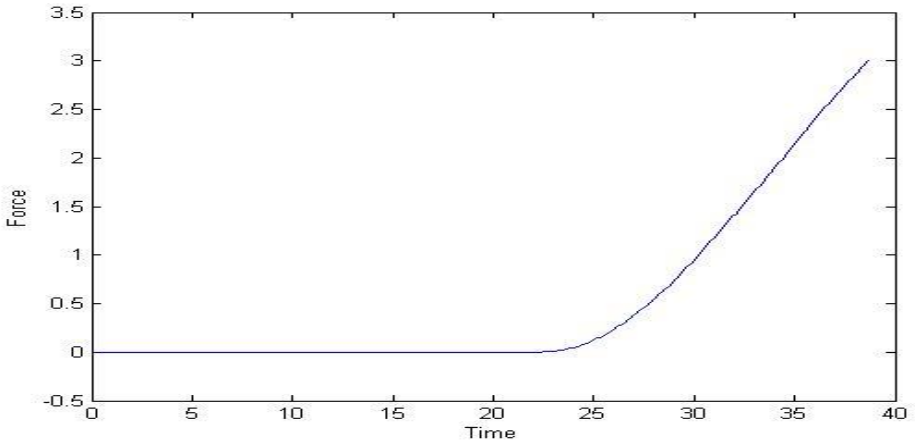

Figure 36 - Compression force F as a function of time, applied during the test. (Force [N] – Time [s])

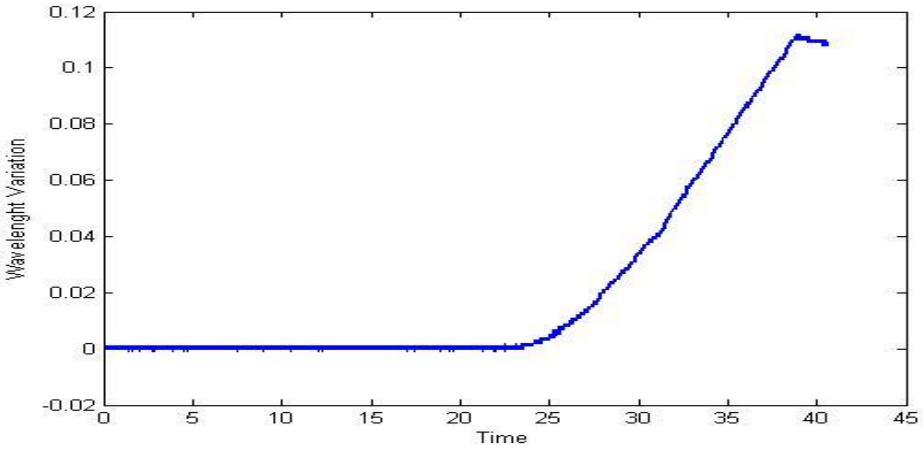

Figure 37 - Change of Bragg wavelength as a function of time, registered by OSA, the applied force was 3N. (Wavelength [nm] – Time [s])

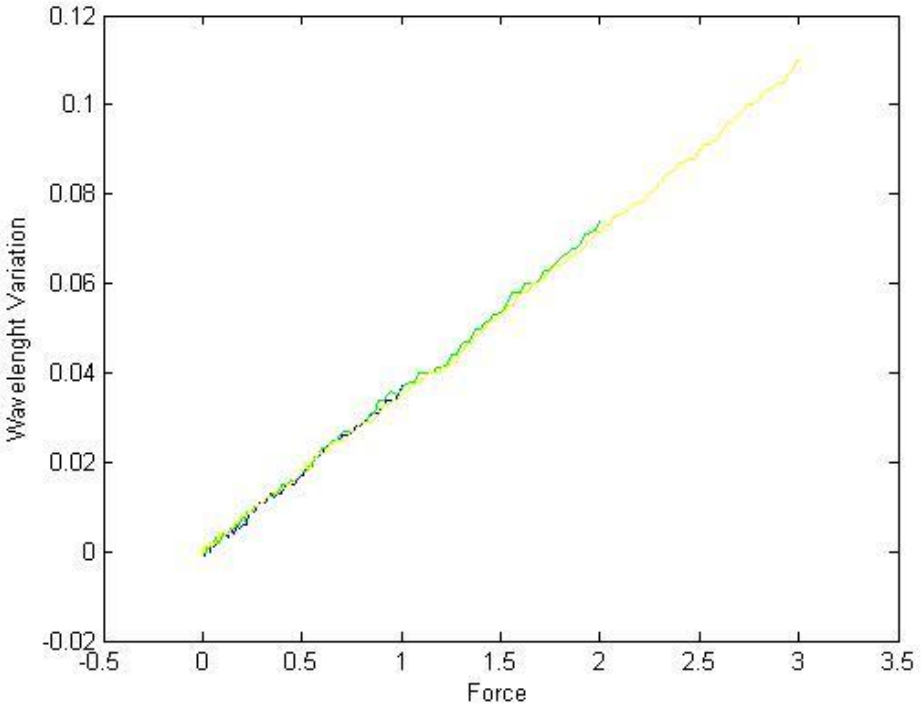

Figure 38 - Repeatable monotonic modulation of wavelength, for FBG 3 as a function of the indentation force F, in the table are shown the trends for 1, 2 and 3N. (Wavelength [nm] – Force [N])

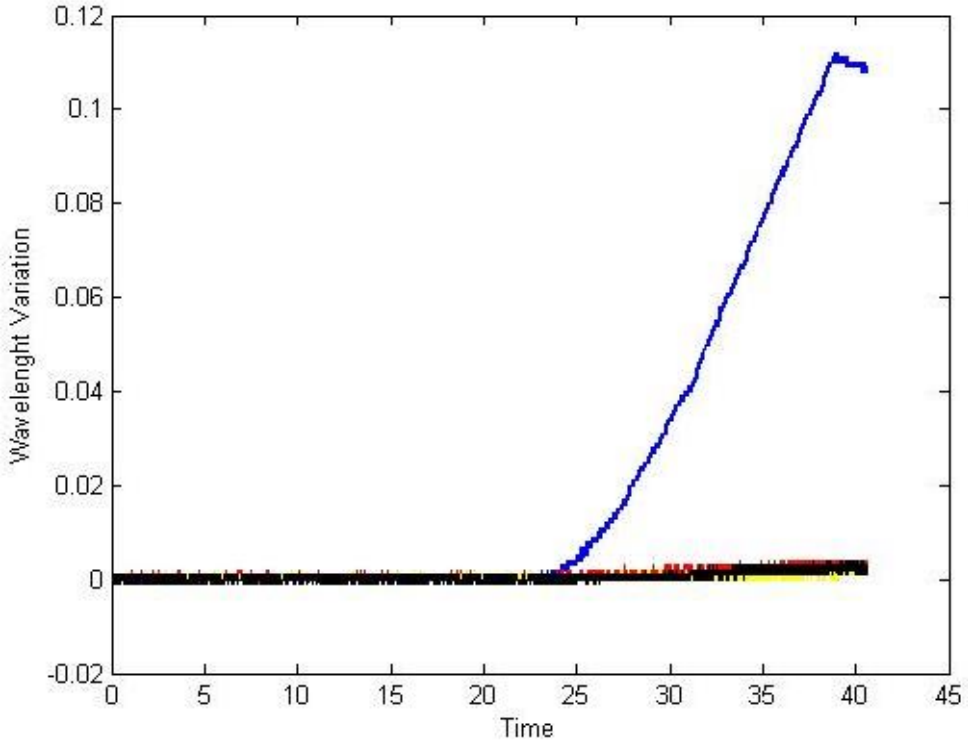

Figure 39 – Change of Bragg wavelength when is applied a force F on the FBG sensor (blue line), and evaluation of the behavior of the 3 adjacent sensors (of the relative cross). (Wavelength [nm] – Time [s])

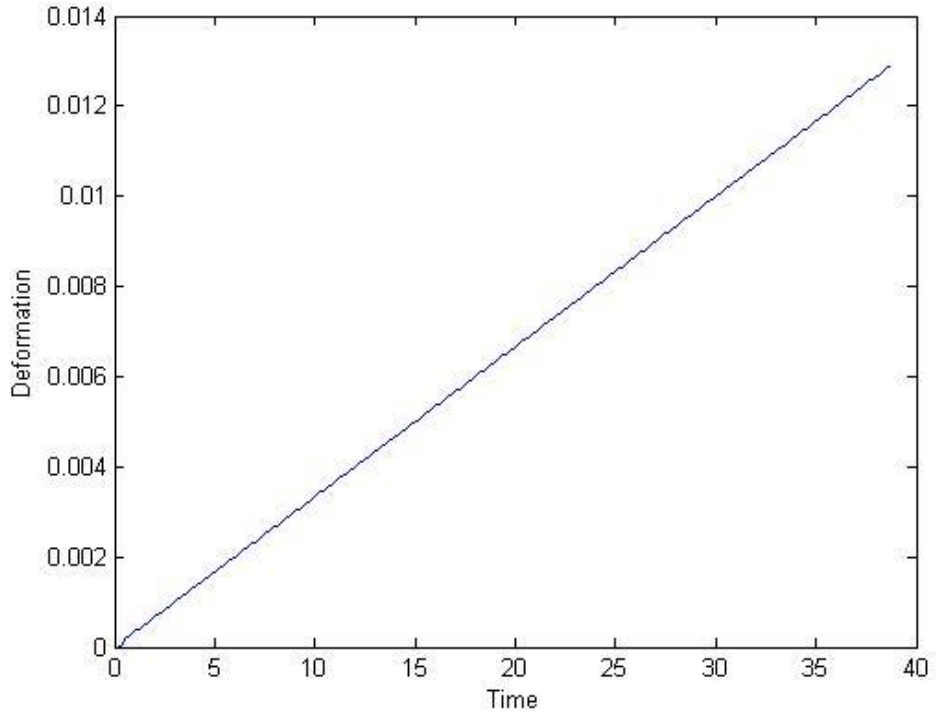

Figure 40 - Deformation as a function of time, applied during the test (Deformation [mm/mm] – Time [s])

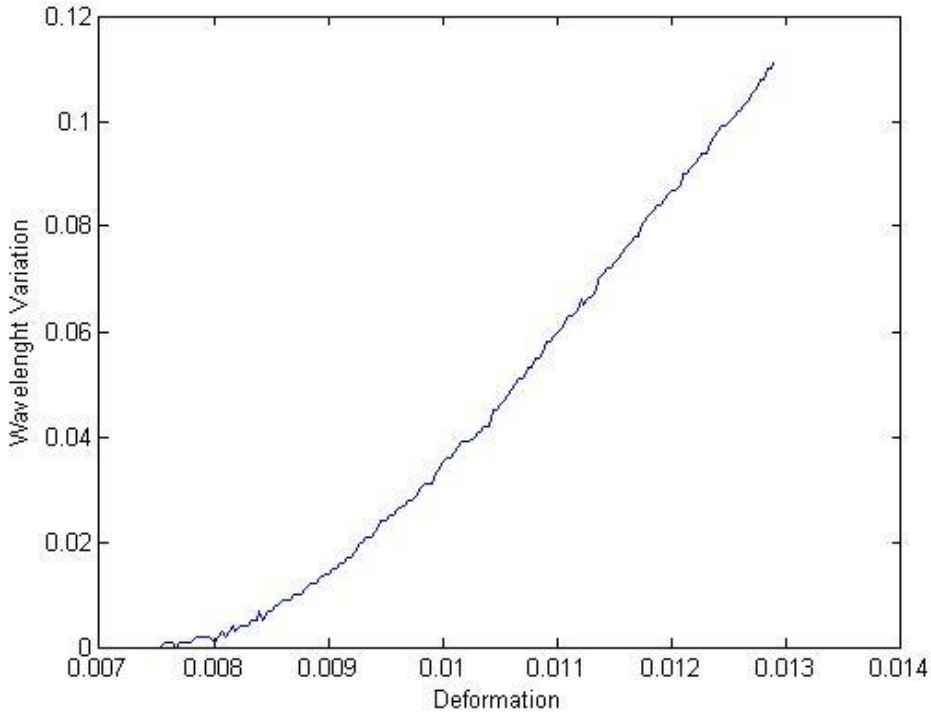

Figure 41 - Change of Bragg wavelength as a function of deformation, registered by OSA, the applied force was 3N. (Wavelength [nm] - Deformation [mm/mm])

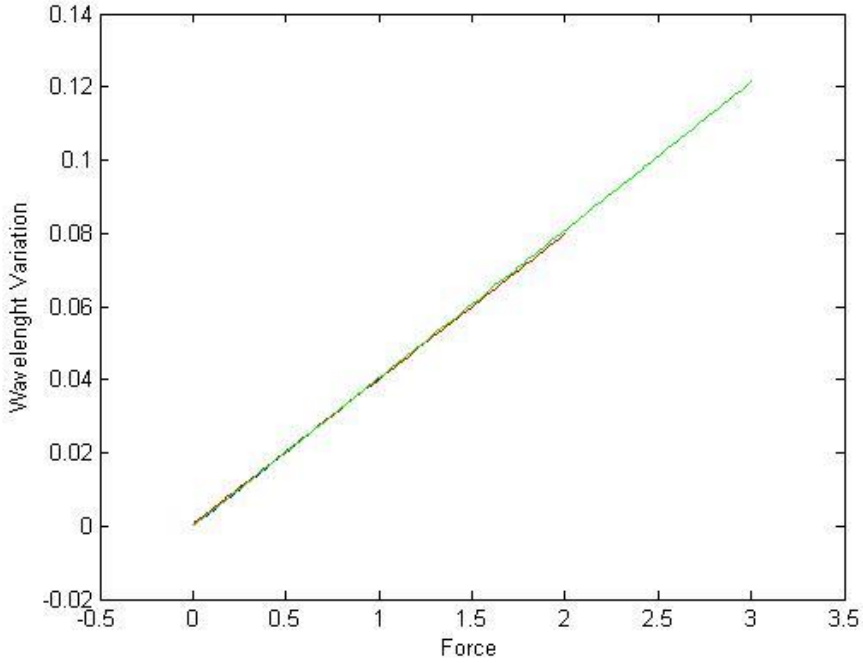

Figure 42 - Change of Bragg wavelength as a function of applied Force, registered by OSA, for sensor 8. In the Figure, we have in different colors all the applied Force 1-2-3N. The lines are obtained by polyfitting with MatLab the curves obtained with the experimental trials (Wavelength [nm] – Force [N]

SENSOR 8	1N (Blue)	2N (Red)	3N (Green)
Angular coefficient	0,040323872 (nm/N)	0,039612159 (nm/N)	0,040414829 (nm/N)
Intercept	-8,76509E-05 nm	0,000541301 nm	2,64747E-05 nm
Correlation coefficient	0,998563345	0,999386906	0,999598758

Figure 43 - Table with the output of sensor 8

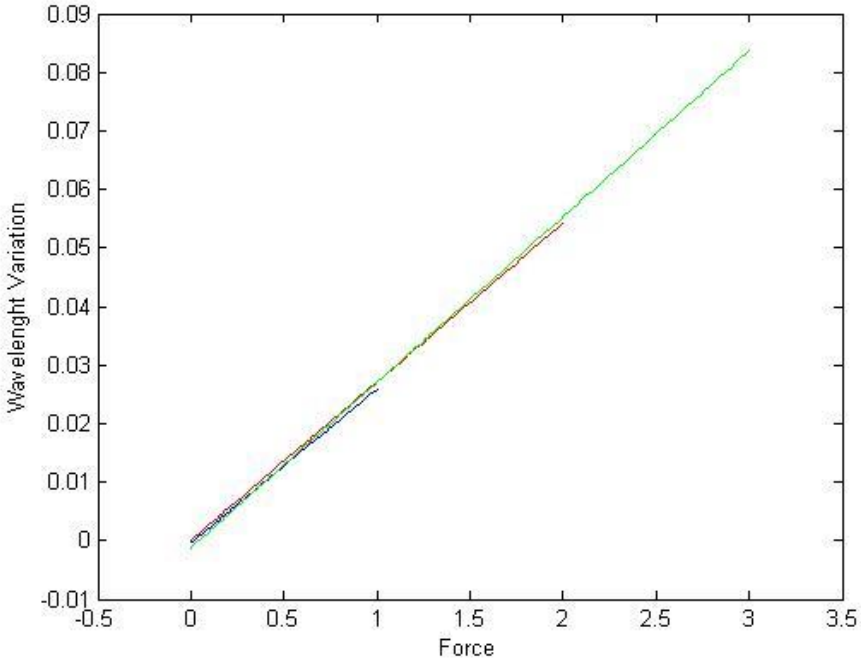

Figure 44 - Change of Bragg wavelength as a function of applied Force, registered by OSA, for sensor 5. In the Figure, we have in different colors all the applied Force 1-2-3N. The lines are obtained by polyfitting with MatLab the curves obtained with the experimental trials (Wavelength [nm] – Force [N]

SENSOR 5	1N (Blue)	2N (Red)	3N (Green)
Angular coefficient	0,026365209 (nm/N)	0,027101072 (nm/N)	0,028265067 (nm/N)
Intercept	-0,000443433 nm	3,96113E-05 nm	-0,001195469 nm
Correlation coefficient	0,993999434	0,99736672	0,996960858

Figure 45 - Table with the output of sensor 5

5 Discussion and conclusion

This study presented the design and preliminary evaluation of a tactile sensor array integrating FBG transducers for hand biomechanical measurements. Its basic working principle, already assessed in the literature of this field, has been further investigated in terms of smart textiles. The sensor had a simple design and fabrication process, requiring: one fiber to house 12 FBGs and Dragon Skin layer to cover and hold the fiber in position, furthermore the polymer has the function of protection of the sensors as well as to distribute the load above the surface of the array. Considering other sensing principles from the well-established ones, such as piezoresistive, piezoelectric and capacitive sensors, to the innovative ones, such as electroactive polymers and fluidic sensors, FBGs offer many advantages. The main added value of FBG based sensors, along with the absence of electromagnetic interferences and MR compatibility, is related to the possibility to increase the number of FBGs within the array. Indeed, as the number of sensors increases wiring issues become relevant in traditional implementations. Conversely, the possibility to integrate a number of FBGs within the same fiber allows reducing the encumbrance of the wiring since a single optical fiber may be enough for all the transducers. Also, another advantage is the wide measurement range in comparison to several tactile sensors developed for robotic or prosthetic purposes [54, 55], which have been characterized within a measurement range typically limited up to 2,5N. A limitation of FBG technology could be represented by the need for temperature compensation, since FBGs are sensitive to both mechanical strain and temperature change, showing a behaviour similar to strain gauges. Therefore, specific designs are invoked to arrange FBG for temperature reference measurement in positions that do not experience strain, and whose change of Bragg wavelength could be only due to temperature changes [56]. Particular configurations aim to compensate the optical output of the other FBGs in the same array, dedicated to strain measurement. On the other hand, under specific design conditions, it is possible to take advantage from this intrinsic feature of FBGs, which can be used to implement a multimodal tactile sensor, providing both strain and temperature information [57, 58].

The encouraging results and the attractive performances of the developed tactile sensor lead to investigate more accurate fabrication processes of the proposed prototype, with

the aim to minimize chirping effect during FBG strain, to control cross-talk among sensors and to evaluate the optimal design for the compensation of temperature influence.

6 Appendix 1 – Experimental data

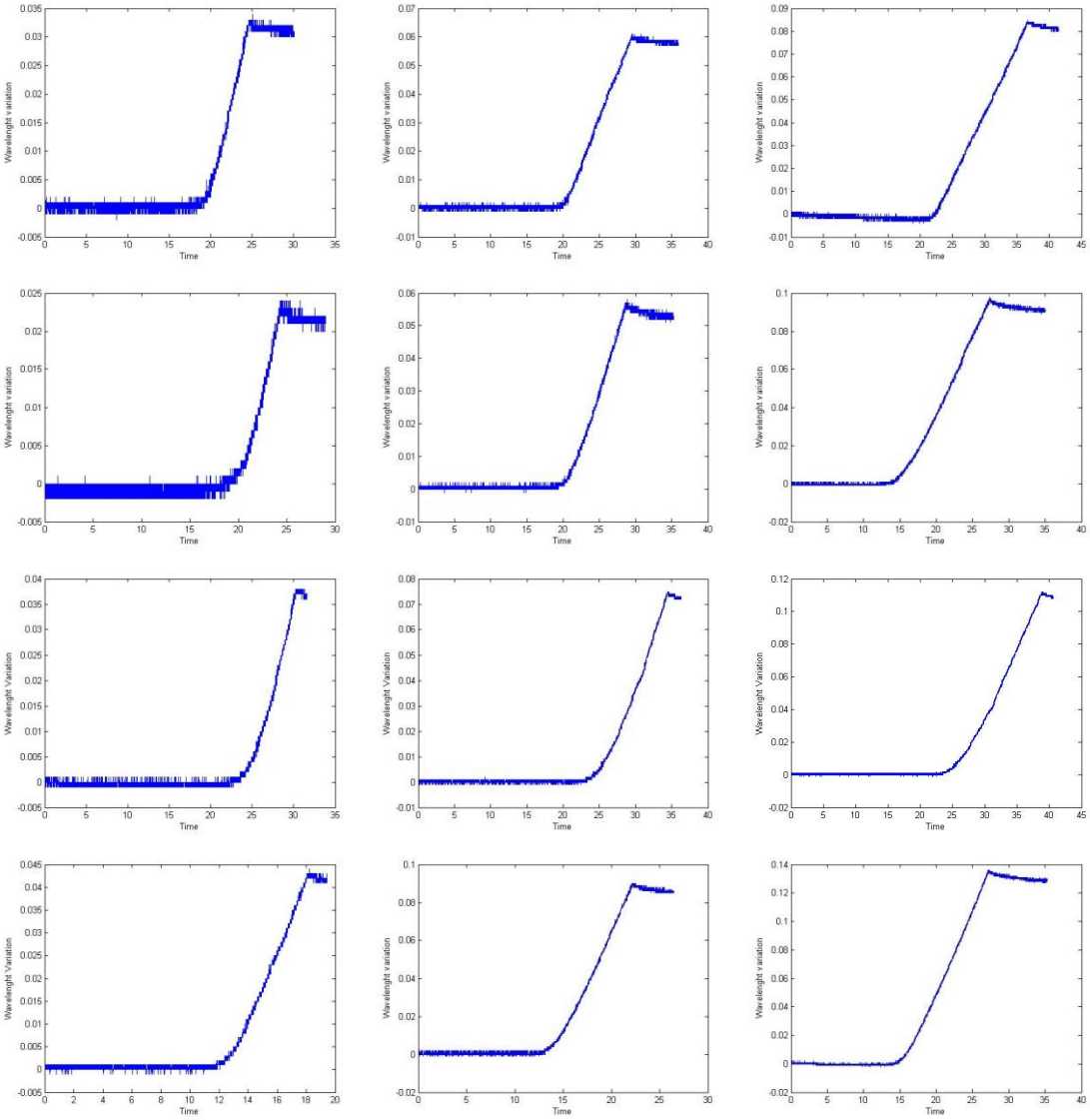

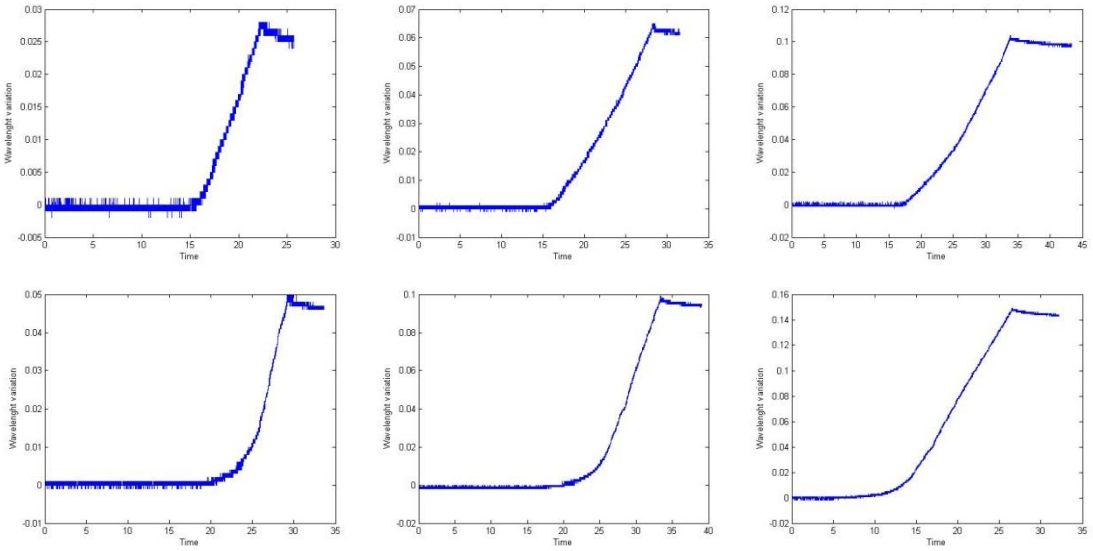

Figure 46 - Change of Bragg wavelength as a function of time, registered by OSA, for sensor 1 to 6. In the first column the applied force is 1N, in the second 2N and in the third 3N. (Wavelength [nm] – Time [s])

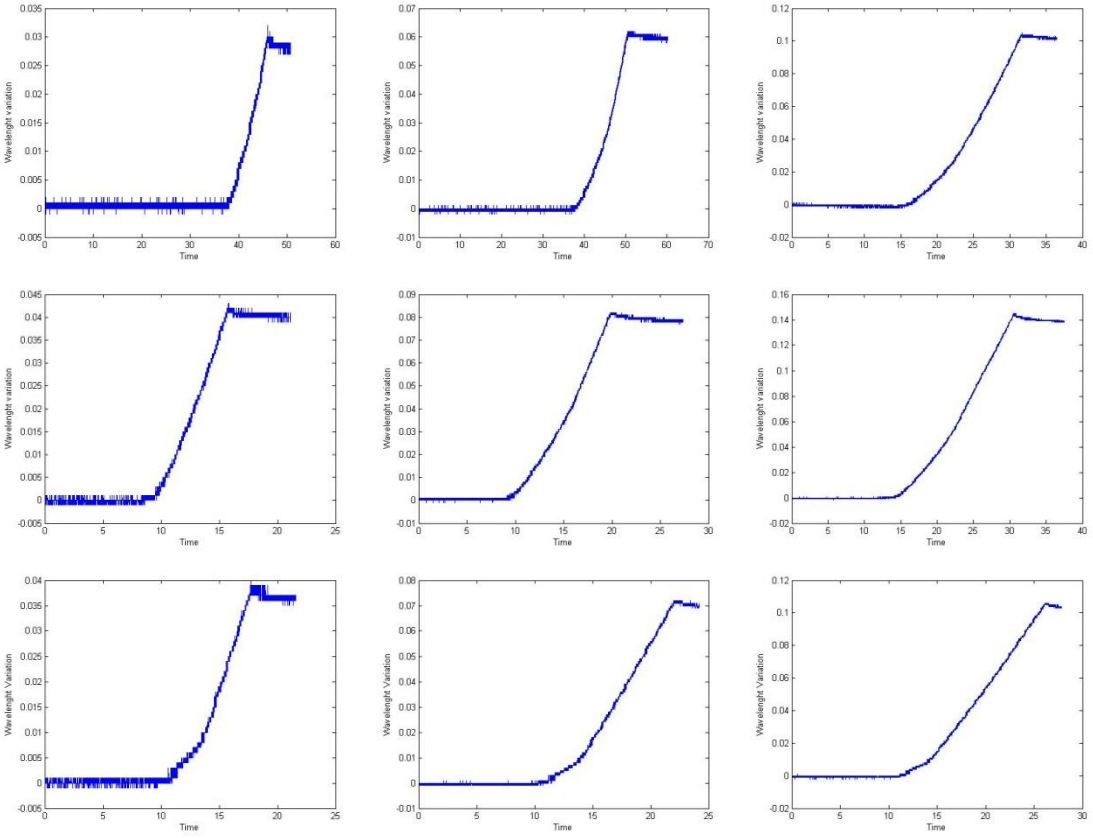

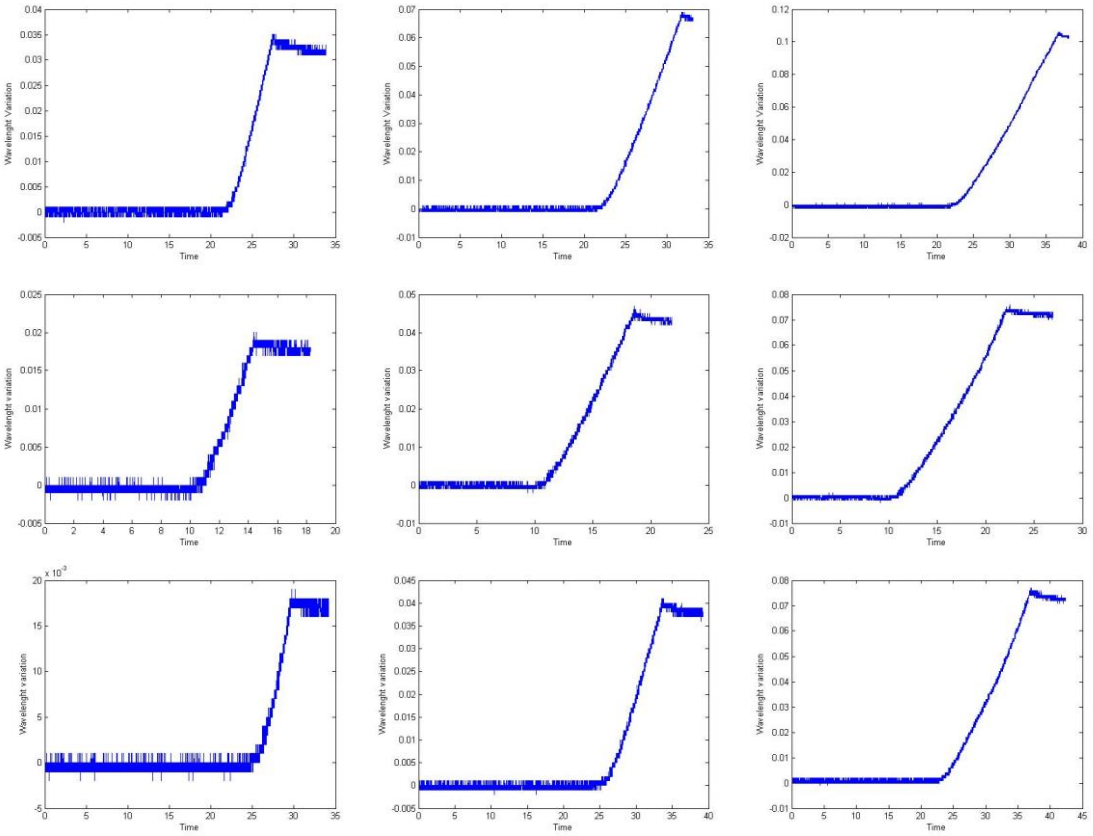

Figure 47 - Change of Bragg wavelength as a function of time, registered by OSA, for sensor 7 to 12. In the first column the applied force is 1N, in the second 2N and in the third 3N. (Wavelength [nm] – Time [s])

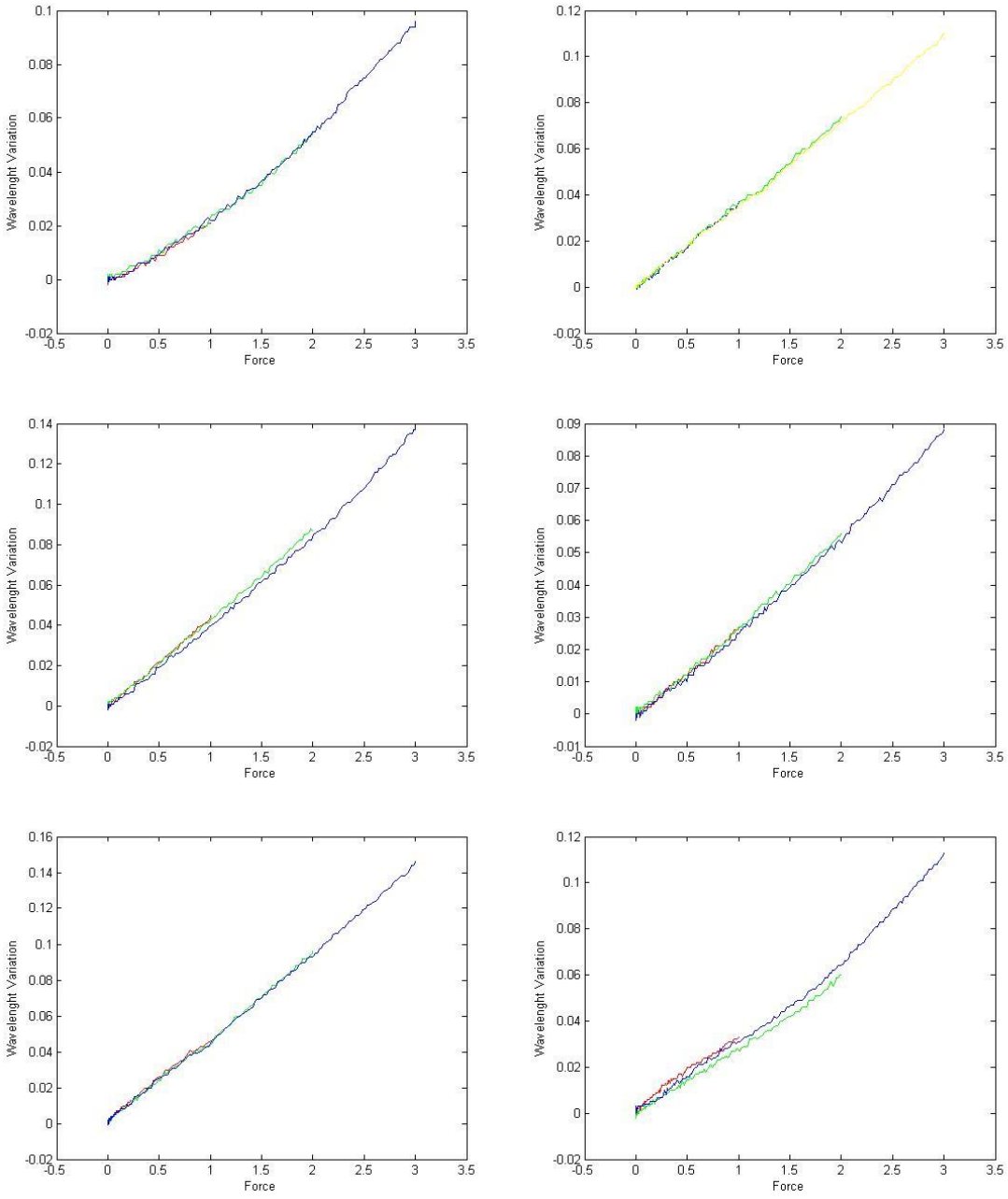

Figure 48 - Change of Bragg wavelength as a function of applied Force, registered by OSA, for sensor 2 to 7. In each figure we have in different colors all the applied Force 1-2-3N. (Wavelength [nm] – Force [N]

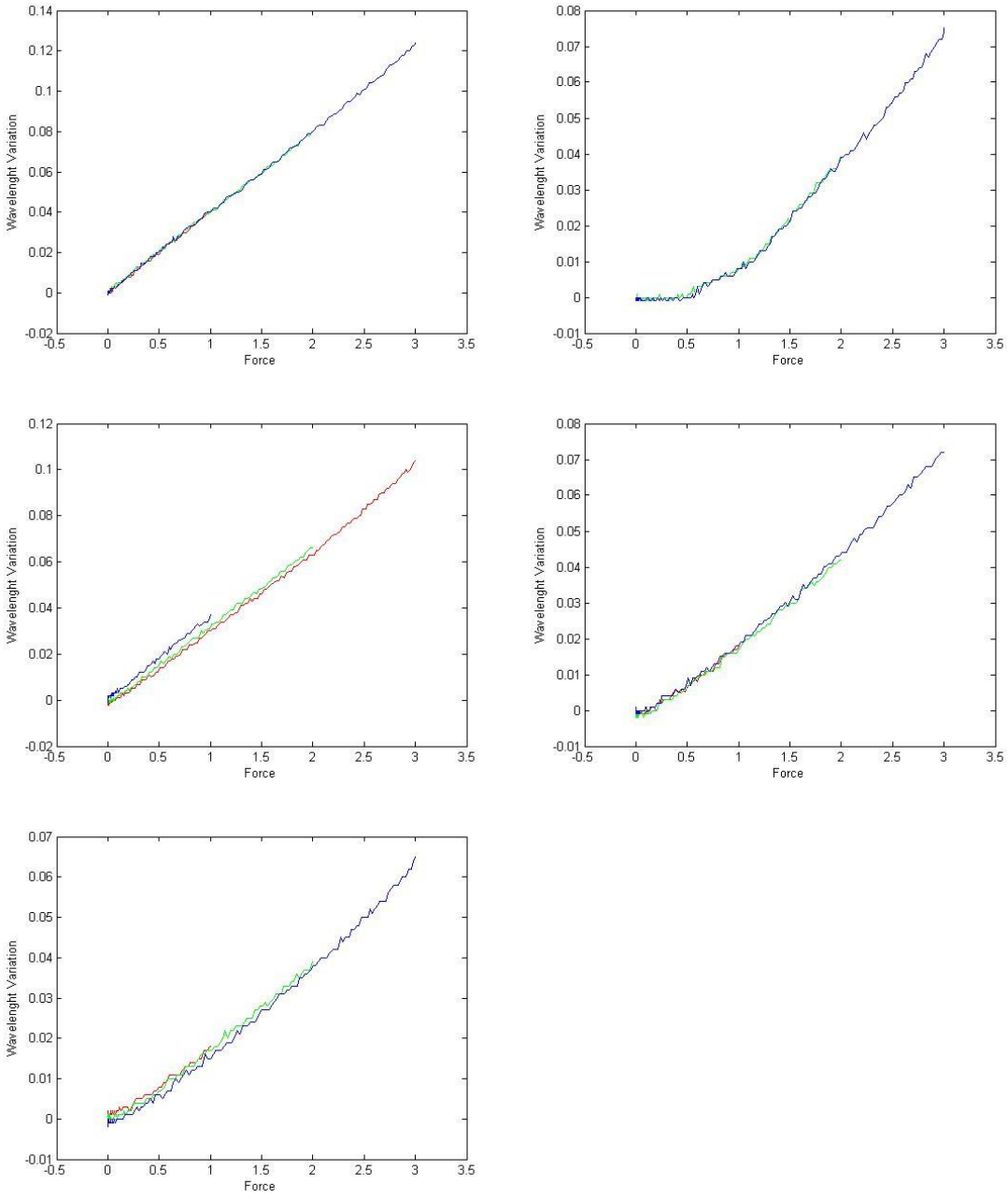

Figure 49 - Change of Bragg wavelength as a function of applied Force, registered by OSA, for sensor 8 to 12. In each figure we have in different colors all the applied Force 1-2-3N. (Wavelength [nm] – Force [N]

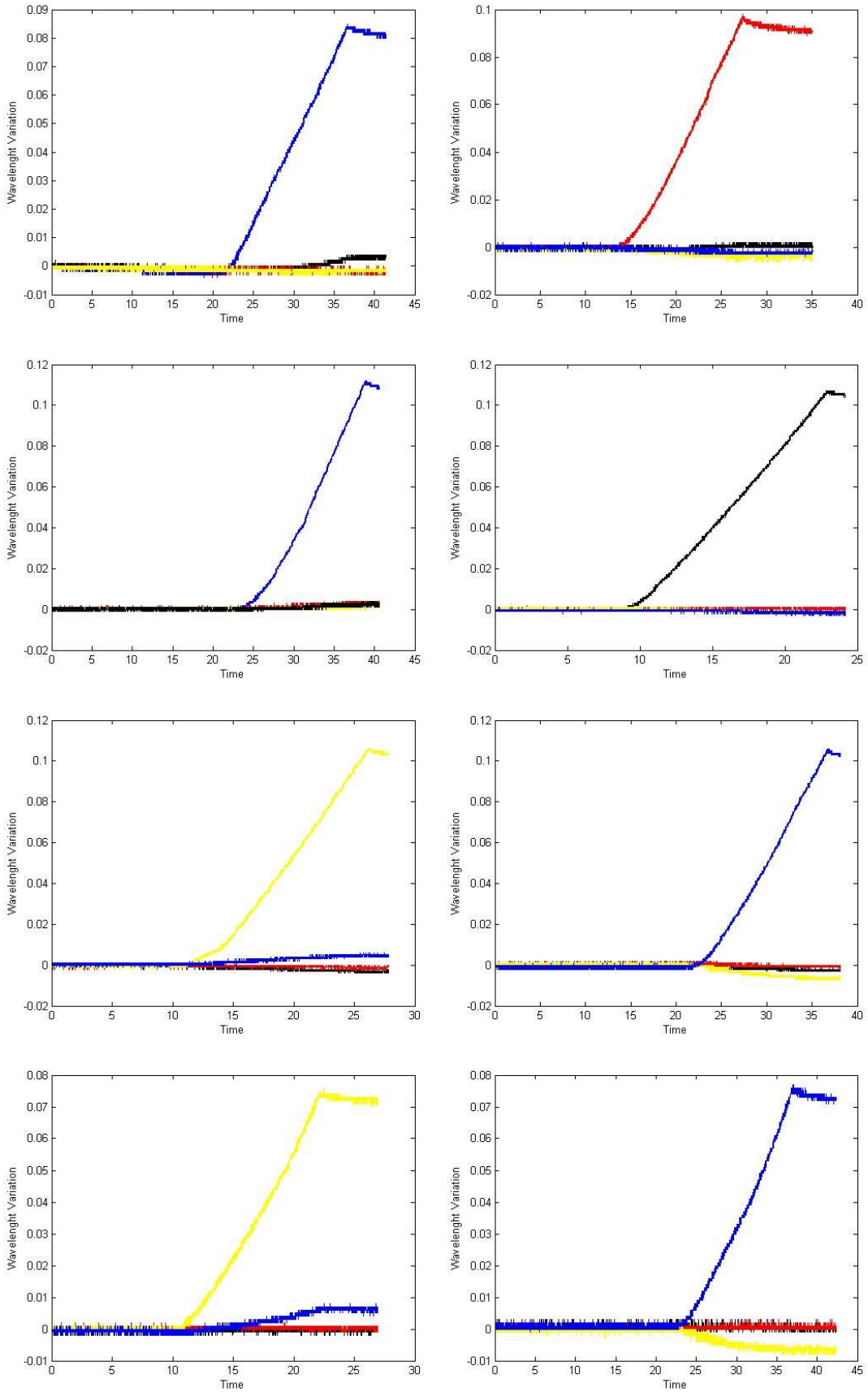

Figure 50 - Change of Bragg wavelength when is applied a force F on the FBG sensor (blue line), and evaluation of the behavior of the 3 adjacent sensors for the first cross and the second cross (Wavelength [nm] – Time [s])

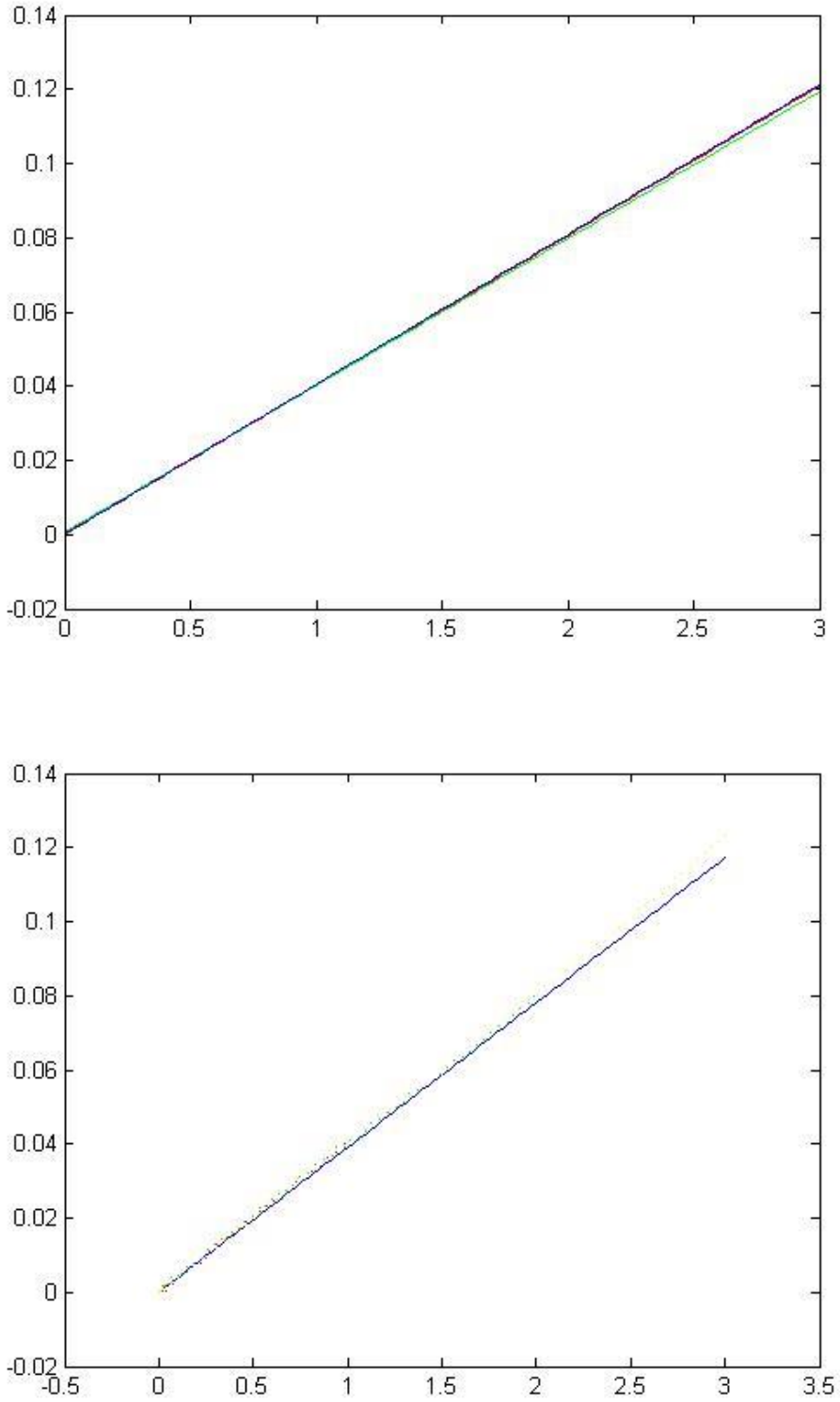

Figure 51 - Change of Bragg wavelength as a function of applied Force, registered by OSA, for sensor 8 . In each figure we have in different colors all the applied Force 1-2-3N. (Wavelength [nm] – Force [N])

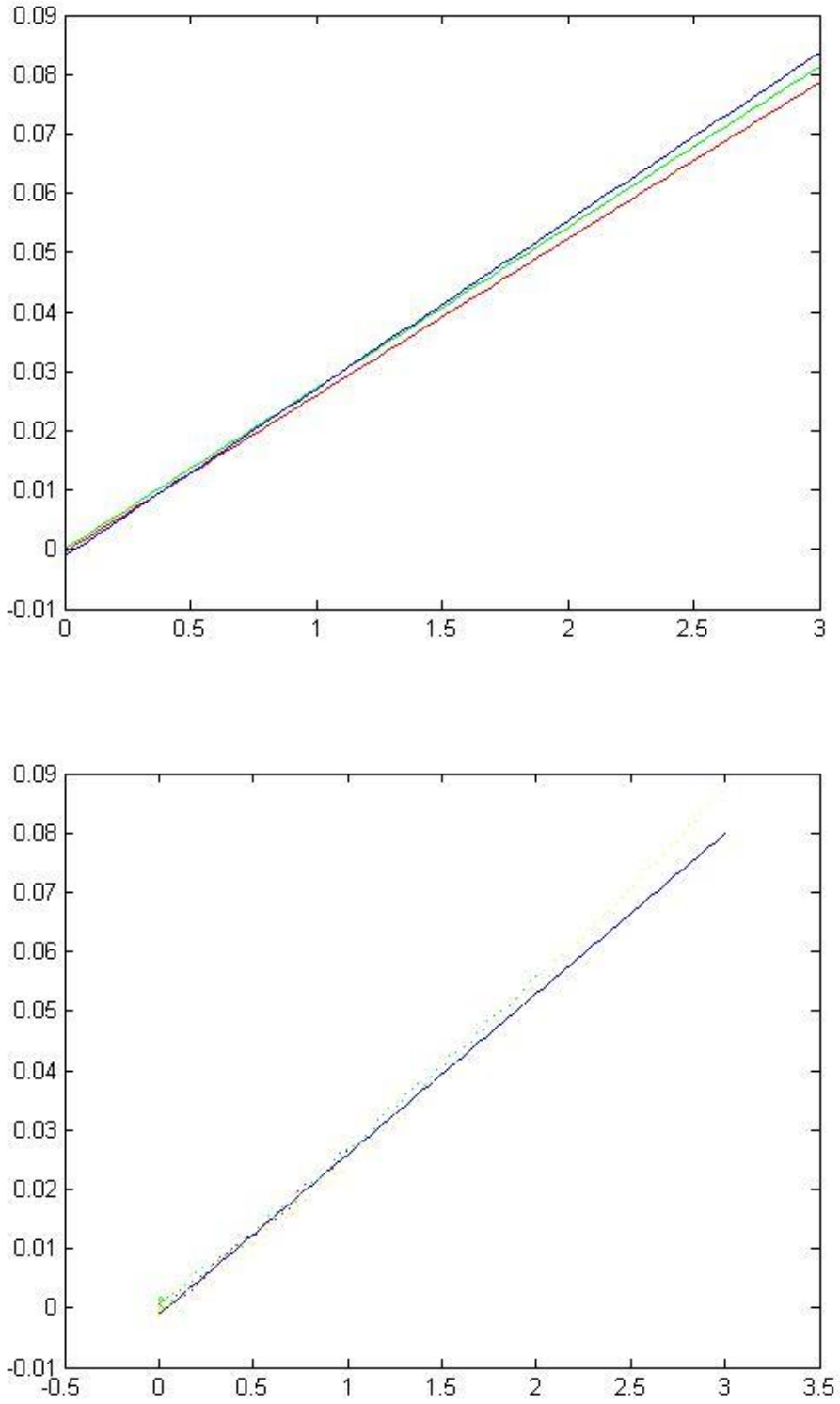

Figure 52 - Change of Bragg wavelength as a function of applied Force, registered by OSA, for sensor 5 . In each figure we have in different colors all the applied Force 1-2-3N. (Wavelength [nm] – Force[N])

```
a = A8 (: ,10);
b = B8 (: ,10);
c = C8 (: ,10);
gn = Prova1NS81 (1:25:3975, 13) - Prova1NS81 (1 , 13);
gn1 = Prova2NS81 (1:25:4950, 13) - Prova2NS81 (1 , 13);
gn2 = Prova3NS81 (1:25:5900, 13) - Prova3NS81 (1 , 13);
p = polyfit (a, gn, 1);
p1 = polyfit (b, gn1, 1);
p2 = polyfit (c, gn2, 1);
yy = polyval (p, a);
T = table (a, gn, yy, gn - yy)
plot (a, yy);
hold on
 yy1 = polyval (p1, b);
T1 = table (b, gn1, yy1, gn1 – yy1)
plot (b, yy1, 'r');
 hold on
 yy2 = polyval (p2, c);
T2 = table (c, gn2, yy2, gn2 – yy2)
plot (c, yy2, 'g' );
```

Figure 53 - MatLab code to obtain the polyfit of the curves

OUTPUT	
Statistical Regression	
R multiplex	0,996995203
R square	0,993999434
R square correct	0,993972159
Standard Error	0,000561498
Observations	222

Variance Analysis

	Dof	*SQ*	*MQ*	*F*	*Significance F*
Regression	1	0,01148981	0,01148981	36443,20835	2,1512E-246
Tot	221	0,011559171			

	Coefficient	*Standard Error*	*Stat t*	*Value of significance*
Intercepts	-0,000443433	4,26287E-05	-10,40221441	7,20544E-21
Variable X 1	0,026365209	0,000138109	190,9010434	2,1512E-246

Figure 54 – Table of the output of the linear regression analysis of the sensor 5 when applied 1N of force

OUTPUT	
Statistical Regression	
R multiplex	0,999281414
R square	0,998563345
R square correct	0,998554194
Standard Error	0,000445682
Observations	159

Variance Analysis

	Dof	*SQ*	*MQ*	*F*	*Significance F*
Regression	1	0,021675733	0,021675733	109124,5919	4,5268E-225
Tot	158	0,021706918			

	Coefficient	*Standard Error*	*Stat t*	*Value of significance*

Intercepts	-8,76509E-05	4,17274E-05	-2,100560713	0,037277551
Variable X 1	0,040323872	0,000122068	330,3401155	4,5268E-225

Figure 55 - Table of the output of the linear regression analysis of the sensor 8 when applied 1N of force

7 References

1. http://epp.eurostat.ec.europa.eu/portal/page/portal/statistics/themes, E.A.f.
2. Inail, Relazione Annuale 2012 del Presidente - Appendice statistica. Luglio 2013.
3. Testo unico sulla salute e sicurezza sul lavoro, in D.lgs. 9 aprile 2008, n.81. 2008: Gazzetta Ufficiale n. 101 del 30 aprile 2008 - Suppl. Ordinario n. 108. p. 329.
4. Colombini, D., E. Occhipinti, and M. Fanti, *Il metodo OCRA per l'analisi e la prevenzione del rischio da movimenti ripetuti.* Milano: Collana Salute e lavoro, Franco Angeli Editore, 2005.
5. Bernard, B.P. and V. Putz-Anderson, *Musculoskeletal disorders and workplace factors: a critical review of epidemiologic evidence for work-related musculoskeletal disorders of the neck, upper extremity, and low back*1997: US Department of Health and Human Services, Public Health Service, Centers for Disease Control and Prevention, National Institute for Occupational Safety and Health Cincinnati, OH, USA.
6. Doyle, C., *Fibre Bragg Grating Sensors-An Introduction to Bragg gratings and interrogation techniques.* Smart Fibres Ltd, 2003: p. 1-5.
7. Grillet, A., et al., *Optical fiber sensors embedded into medical textiles for healthcare monitoring.* Sensors Journal, IEEE, 2008. **8**(7): p. 1215-1222.
8. Jeanne, M., et al. *OFSETH: optical fibre embedded into technical textile for healthcare, an efficient way to monitor patient under magnetic resonance imaging*. in *Engineering in Medicine and Biology Society, 2007. EMBS 2007. 29th Annual International Conference of the IEEE*. 2007. IEEE.
9. Cempini, M., M. Cortese, and N. Vitiello, *A Powered Finger-Thumb Wearable Hand Exoskeleton With Self-Aligning Joint Axes.* Mechatronics, IEEE/ASME Transactions on, 2015. **20**(2): p. 705-716.
10. Yan, T., et al., *Review of assistive strategies in powered lower-limb orthoses and exoskeletons.* Robotics and Autonomous Systems, 2015. **64**: p. 120-136.
11. Raspopovic, S., et al., *Restoring Natural Sensory Feedback in Real-Time Bidirectional Hand Prostheses.* Science Translational Medicine, 2014. **6**(222): p. 222ra19.
12. Castano, L.M. and A.B. Flatau, *Smart fabric sensors and e-textile technologies: a review.* Smart Materials and Structures, 2014. **23**(5): p. 053001.
13. Meyer, J., et al., *Design and modeling of a textile pressure sensor for sitting posture classification.* Sensors Journal, IEEE, 2010. **10**(8): p. 1391-1398.
14. Hui, Z., et al. *Pressure sensing fabric*. in *MRS Proceedings*. 2006. Cambridge Univ Press.
15. Li, L.-F. and Y.-S. Ding. *Design and Analysis of Parallel Woven Structure-Based Flexible Resistive Pressure Sensor*. in *Bioinformatics and Biomedical Engineering, 2009. ICBBE 2009. 3rd International Conference on*. 2009. IEEE.
16. Inaba, M., et al. *A full-body tactile sensor suit using electrically conductive fabric and strings*. in *Intelligent Robots and Systems' 96, IROS 96, Proceedings of the 1996 IEEE/RSJ International Conference on*. 1996. IEEE.
17. Massaroni, C., P. Saccomandi, and E. Schena, *Medical Smart Textiles Based on Fiber Optic Technology: An Overview.* Journal of functional biomaterials, 2015. **6**(2): p. 204-221.
18. da Silva, A.F., et al., *FBG sensing glove for monitoring hand posture.* Sensors Journal, IEEE, 2011. **11**(10): p. 2442-2448.
19. Wehrle, G., et al., *A fibre optic Bragg grating strain sensor for monitoring ventilatory movements.* Measurement Science and Technology, 2001. **12**(7): p. 805.
20. Augousti, A., F. Maletras, and J. Mason, *Improved fibre optic respiratory monitoring using a figure-of-eight coil.* Physiological measurement, 2005. **26**(5): p. 585.
21. Witt, J., et al., *Medical textiles with embedded fiber optic sensors for monitoring of respiratory movement.* Sensors Journal, IEEE, 2012. **12**(1): p. 246-254.

22. Narbonneau, F., et al. *FBG-based smart textiles for continuous monitoring of respiratory movements for healthcare applications*. in *e-Health Networking Applications and Services (Healthcom), 2010 12th IEEE International Conference on*. 2010. IEEE.
23. Silva, A., et al., *Simultaneous cardiac and respiratory frequency measurement based on a single fiber Bragg grating sensor.* Measurement Science and Technology, 2011. **22**(7): p. 075801.
24. Carmo, J.P., et al., *Application of fiber Bragg gratings to wearable garments.* Sensors Journal, IEEE, 2012. **12**(1): p. 261-266.
25. ukasz Dziuda, Ł., et al., *Fiber Bragg grating-based sensor for monitoring respiration and heart activity during magnetic resonance imaging examinations.* Journal of biomedical optics, 2013. **18**(5): p. 057006-057006.
26. Dziuda, L., et al., *Monitoring respiration and cardiac activity using fiber Bragg grating-based sensor.* Biomedical Engineering, IEEE Transactions on, 2012. **59**(7): p. 1934-1942.
27. Dziuda, L., M. Krej, and F. Skibniewski, *Fiber Bragg grating strain sensor incorporated to monitor patient vital signs during MRI.* Sensors Journal, IEEE, 2013. **13**(12): p. 4986-4991.
28. Krej, M., L. Dziuda, and F. Skibniewski, *A method of detecting heartbeat locations in the ballistocardiographic signal from the fiber-optic vital signs sensor.* 2015.
29. Allsop, T., et al., *Respiratory function monitoring using a real-time three-dimensional fiber-optic shaping sensing scheme based upon fiber Bragg gratings.* Journal of biomedical optics, 2012. **17**(11): p. 117001-117001.
30. Li, H., et al., *Wearable sensors in intelligent clothing for measuring human body temperature based on optical fiber Bragg grating.* Optics Express, 2012. **20**(11): p. 11740-11752.
31. Silva, A.F.d., et al., *A smart skin PVC foil based on FBG sensors for monitoring strain and temperature.* Industrial Electronics, IEEE Transactions on, 2011. **58**(7): p. 2728-2735.
32. Silva, A., et al. *Manufacturing technology for flexible optical sensing foils*. in *Industrial Electronics, 2009. IECON'09. 35th Annual Conference of IEEE*. 2009. IEEE.
33. Kanellos, G.T., et al., *Two dimensional polymer-embedded quasi-distributed FBG pressure sensor for biomedical applications.* Optics Express, 2010. **18**(1): p. 179-186.
34. Watanabe, K., K. TAJIMA, and Y. KUBOTA, *Macrobending characteristics of a hetero-core splice fiber optic sensor for displacement and liquid detection.* IEICE transactions on electronics, 2000. **83**(3): p. 309-314.
35. Nishiyama, M., H. Sasaki, and K. Watanabe, *A deformation sensitive pad-structure embedded with hetero-core optic fiber sensors.* Sensors and Actuators A: Physical, 2007. **136**(1): p. 205-211.
36. Lekholm, A. and L. Lindström, *Optoelectronic transducer for intravascular measurements of pressure variations.* Medical and biological engineering, 1969. **7**(3): p. 333-335.
37. Totsu, K., Y. Haga, and M. Esashi, *Ultra-miniature fiber-optic pressure sensor using white light interferometry.* Journal of Micromechanics and Microengineering, 2005. **15**(1): p. 71.
38. Babchenko, A., et al., *Fiber optic sensor for the measurement of respiratory chest circumference changes.* Journal of biomedical optics, 1999. **4**(2): p. 224-229.
39. Narbonneau, F., et al. *Smart textile embedding optical fibre sensors for healthcare monitoring during MRI*. in *Advances in Science and Technology*. 2009. Trans Tech Publ.
40. Krehel, M., et al., *Characterization of flexible copolymer optical fibers for force sensing applications.* Sensors, 2013. **13**(9): p. 11956-11968.
41. Tognetti, A., et al., *Body segment position reconstruction and posture classification by smart textiles.* Transactions of the Institute of Measurement and Control, 2007. **29**(3-4): p. 215-253.

42. Lee, J., et al., *Conductive Fiber-Based Ultrasensitive Textile Pressure Sensor for Wearable Electronics.* Advanced Materials, 2015.
43. Dobrzynska, J.A. and M.A. Gijs, *Flexible polyimide-based force sensor.* Sensors and Actuators A: Physical, 2012. **173**(1): p. 127-135.
44. Boulogne, F., et al., *Suppression of the Rayleigh–Plateau instability on a vertical fibre coated with wormlike micelle solutions.* Soft Matter, 2013. **9**(32): p. 7787-7796.
45. Macha, S.F., et al., *Silver cluster interferences in matrix-assisted laser desorption/ionization (MALDI) mass spectrometry of nonpolar polymers.* Journal of the American Society for Mass Spectrometry, 2001. **12**(6): p. 732-743.
46. Park, M., et al., *Highly stretchable electric circuits from a composite material of silver nanoparticles and elastomeric fibres.* Nature nanotechnology, 2012. **7**(12): p. 803-809.
47. Carbonaro, N., et al., *Exploiting wearable goniometer technology for motion sensing gloves.* Biomedical and Health Informatics, IEEE Journal of, 2014. **18**(6): p. 1788-1795.
48. Bland, J.M. and D. Altman, *Statistical methods for assessing agreement between two methods of clinical measurement.* The lancet, 1986. **327**(8476): p. 307-310.
49. Silva, A.F.d., et al., *PVC smart sensing foil for advanced strain measurements.* Sensors Journal, IEEE, 2010. **10**(6): p. 1149-1155.
50. http://www.fbgs.com.
51. http://www.micronoptics.com.cn/pdfs/si425.pdf.
52. http://www.ibsenphotonics.com/products/interrogation-monitors/i-mon-high-speed/i-mon-256-512-high-speed/.
53. http://www.instron.com/en.
54. Oddo, C.M., et al. *A biomimetic MEMS-based tactile sensor array with fingerprints integrated in a robotic fingertip for artificial roughness encoding*. in *Robotics and Biomimetics (ROBIO), 2009 IEEE International Conference on*. 2009. IEEE.
55. Beccai, L., et al., *Design and fabrication of a hybrid silicon three-axial force sensor for biomechanical applications.* Sensors and Actuators A: Physical, 2005. **120**(2): p. 370-382.
56. Zhang, Z., et al., *Sensitivity enhancement of strain sensing utilizing a differential pair of fiber bragg gratings.* Sensors, 2012. **12**(4): p. 3891-3900.
57. Yang, Y.-J., et al., *A 32× 32 temperature and tactile sensing array using PI-copper films.* The International Journal of Advanced Manufacturing Technology, 2010. **46**(9-12): p. 945-956.
58. Castelli, F., *An integrated tactile-thermal robot sensor with capacitive tactile array.* Industry Applications, IEEE Transactions on, 2002. **38**(1): p. 85-90.

Ringraziamenti

Desidero ringraziare Dr.Calogero Oddo, responsabile di questa tesi, per la grande disponibilità e cortesia dimostratemi, e per tutto l'aiuto fornito durante la stesura. Un sentito ringraziamento al Professor Cappa che mi ha permesso di raggiungere questo traguardo. Desidero inoltre ringraziare Emiliano Schena e Paola Saccomandi del Campus BioMedico, per tutto quanto hanno fatto per me. Un ringraziamento ai compagni del Sant'Anna, Francesca, Renato, Domenico, Alice, Angela e Ilaria per essermi stati vicini durante tutto il periodo di Tesi.

Ovviamente l'ultimo e più importante ringraziamento va ad Elena e alla mia famiglia.